NASA TECHNICAL MEMORANDUM

NASA TM X-73,146

NASA TM X-73,146

ANALYTICAL DISPLAY DESIGN FOR FLIGHT TASKS CONDUCTED UNDER INSTRUMENT METEOROLOGICAL CONDITIONS

Ronald A. Hess

Ames Research Center
Moffett Field, Calif. 94035

August 1976

1. Report No.	2. Government Accession No.	3. Recipient's Catalog No.
NASA TM X-73,146		

4. Title and Subtitle	5. Report Date
ANALYTICAL DISPLAY DESIGN FOR FLIGHT TASKS CONDUCTED UNDER INSTRUMENT METEOROLOGICAL CONDITIONS	6. Performing Organization Code

7. Author(s)	8. Performing Organization Report No.
Ronald A. Hess*	A-6636
	10. Work Unit No. 513-54-01
9. Performing Organization Name and Address	11. Contract or Grant No.
NASA-Ames Research Center Moffett Field, California 94035	
	13. Type of Report and Period Covered
12. Sponsoring Agency Name and Address	Technical Memorandum
National Aeronautics and Space Administration Washington, D.C. 20546	14. Sponsoring Agency Code

15. Supplementary Notes

*On assignment from Naval Postgraduate School, Monterey, Calif.

16. Abstract

A relatively straightforward, nearly algorithmic procedure for deriving model-based, pilot-centered display requirements is presented. The optimal or control theoretic pilot model serves as the backbone of the design methodology, which is specifically directed toward the synthesis of head-down, electronic, cockpit display formats. Some novel applications of the optimal pilot model are discussed, including the generation of numerical pilot opinion ratings of vehicle handling qualities via the Cooper-Harper rating scale. An analytical design example is offered which defines a format for the electronic display to be used in a UH-1H helicopter in a landing approach task involving longitudinal and lateral degrees of freedom. It is demonstrated that the design procedure offers a rational means for generating candidate display formats and flight director laws for simulator evaluation.

17. Key Words (Suggested by Author(s))	18. Distribution Statement
Display design Pilot modeling	Unlimited STAR Category - 08

19. Security Classif. (of this report)	20. Security Classif. (of this page)	21. No. of Pages	22. Price*
Unclassified	Unclassified	52	$4.25

*For sale by the National Technical Information Service, Springfield, Virginia 22161

CONTENTS

LIST OF TABLES

LIST OF FIGURES

SYMBOLS

$\underline{A}$, $\underline{B}$, $\underline{C}$	general system matrices
d_i	ith flight director signal
E[a]	expected value of [a]
$\underline{F}$	general system matrix
$f_{a,\dot{a}}$	fraction of attention devoted to displayed quantity a and its perceived derivative $\dot{a}$ (equivalent to f_k)
f_c	fraction of attention devoted to control task as a whole
f_k	fraction of attention devoted to kth displayed quantity and its perceived derivative in subtask s
f_s	fraction of attention devoted to subtask s
f_{lat}	fraction of attention devoted to lateral subtask (equivalent to f_s)
f_{long}	fraction of attention devoted to longitudinal subtask (equivalent to f_s)
$\hat{f}(a)$	amplitude-dependent, pure-gain describing function for a threshold-type nonlinearity associated with the variable (a)
$\underline{G}$, $\underline{H}$	general system matrices
h	deviation from glide slope, m
h_{ij}	pilot transfer function between ith control motion u_i and jth observed variable z_j', m/rad or m/(rad/sec)
I_{ab}	product (or moment) of inertia between a and b vehicle axes, kg-m^2
J	index of performance
J_{lat}	index of performance for lateral subtask
J_{long}	index of performance for longitudinal subtask
L	moment about vehicle x axis, N • m
L_{u_g}	longitudinal turbulence characteristic length, m
L_{v_g}	lateral turbulence characteristic length, m
L_{w_g}	vertical turbulence characteristic length, m

M	moment about vehicle y axis, N • m
m	vehicle mass, kg
N	moment about vehicle z axis, N • m
p	vehicle roll rate, $d\phi/dt$, rad/sec
$\underline{Q}$	system output weighting matrix
q	vehicle pitch rate, $d\theta/dt$, rad/sec
$\underline{R}$	system control weighting matrix
$R(J)_s$	pilot opinion rating function expressed in rating scale s
r	vehicle yaw rate, $d\psi/dt$, rad/sec
T_N	neuromuscular time constant, sec
U_0	vehicle trim groundspeed, m/sec
u	component of vehicle perturbation velocity in x axis, m/sec
u_g	longitudinal turbulence velocity, m/sec
$\underline{u}$	optimal control vector
v	component of vehicle perturbation velocity in y axis, m/sec
v_g	lateral turbulence velocity, m/sec
$\underline{v}$	observation noise vector
$\underline{v}_m$	motor noise vector
w	component of vehicle perturbation velocity in z axis, m/sec
w_g	vertical turbulence velocity, m/sec
$\underline{w}$	white noise vector
X	component of aerodynamic/propulsive force in x axis, N
$\underline{x}$	system state vector
$\hat{\underline{x}}$	estimate of system state vector
xyz	vehicle stability axis system
Y	component of aerodynamic/propulsive force in y axis, N

$\underline{y}$	system output vector
Z	component of aerodynamic/propulsive force in z axis, N
$\underline{z}$	observation vector
$\underline{z}'$	observation vector without observation noise
$\underline{\Gamma}$	general system matrix
γ	longitudinal flight path angle error
δ_A	lateral cyclic motion, m (measured at pilot's hand)
δ_C	collective motion, m (measured at pilot's hand)
δ_E	longitudinal cyclic motion, m (measured at pilot's hand)
δ_{E_a}	longitudinal cyclic stability augmentation system input (in parallel with pilot's δ_E input), m
δ_P	pedal motion, m (measured at pilot's foot)
$\delta( )$	Dirac delta function
θ	vehicle pitch deviation from trim, rad
ρ	noise signal ratio associated with "full attention" to a display indicator
ρ'	noise signal ratio for motor noise
ρ_k	noise signal ratio for kth displayed variable and its observed derivative when attention is being shared
σ	lateral flight path angle error, rad
σ_a	root-mean-square (rms) value of variable a
$\Phi_{u_g u_g}$	power spectral density of longitudinal turbulence velocity u_g, m^2/rad
$\Phi_{v_g v_g}$	power spectral density of lateral turbulence velocity v_g, m^2/rad
$\Phi_{w_g w_g}$	power spectral density of vertical turbulence velocity w_g, m^2/rad
ϕ	vehicle roll angle, rad
ψ	vehicle heading deviation from trim, rad
ω	frequency, rad/sec

ANALYTICAL DISPLAY DESIGN FOR FLIGHT TASKS CONDUCTED UNDER INSTRUMENT METEOROLOGICAL CONDITIONS

Ronald A. Hess*

Ames Research Center

SUMMARY

A relatively straightforward, nearly algorithmic procedure for deriving model-based, pilot-centered display requirements is presented. The optimal or control theoretic pilot model serves as the backbone of the design methodology, which is specifically directed toward the synthesis of head-down, electronic, cockpit display formats. Some novel applications of the optimal pilot model are discussed, including the generation of numerical pilot opinion ratings of vehicle handling qualities via the Cooper-Harper rating scale. An analytical design example is offered which defines a format for the electronic display to be used in a UH-1H helicopter in a landing approach task involving longitudinal and lateral degrees of freedom. It is demonstrated that the design procedure offers a rational means for generating candidate display formats and flight director laws for simulator evaluation.

INTRODUCTION

The design of aircraft cockpit displays tends to be a mixture of common sense, supportive data from simulation, and finally, flight experience. In the past, technology has constrained the display designer to use of electromechanical instruments to provide information appropriate for the vehicle and task at hand. The constraint of economy has, in addition, led to the production of only a limited variety of rather standard flight instruments. With these facts in mind, it is not too surprising to find that the guidance and control instrumentation of a modern, fixed-wing, jet transport, differs little from that of a modern, instrument-certified light helicopter, despite the fact that the vehicles differ drastically in design and capability.

This decade, however, has seen increased application of electronic displays in the cockpit. These devices allow the display designer comparative freedom in plying his trade. The electronic devices can be roughly categorized as head-up or head-down in nature. In the former category, information is presented directly over a portion of the visual field. In the latter group, television-type raster displays, or stroke-written cathode ray tubes (CRT's) are prominent.

---

*On assignment from Naval Postgraduate School, Monterey, California.

The modern electronic displays show potential for alleviating the display problems associated with the operation of vertical/short takeoff and landing (V/STOL) aircraft in instrument meteorological conditions (IMC) (ref. 1). The capabilities of these devices, however, have often outstripped the designer's ability to use them in a rational manner. Typical of the problems which develop are overlapping and/or confusing symbology resulting from an attempt to provide too much information in too small a display area. This difficulty is particularly evident in stroke-written, black and white, CRT displays (ref. 2).

Paramount to proper utilization of electronic displays is a method for determining pilot-centered display requirements. As stated in reference 3, display design should be viewed fundamentally as a guidance and control problem which has interactions with the designer's knowledge of human psychomotor activity. Here, psychomotor activity relates to muscular action ensuing from conscious mental activity. From this standpoint, reliable analytical models of human pilots as information processors and controllers have provided valuable insight into the display design process (refs. 3-6). Pursuing this approach, the research described herein is aimed at developing and demonstrating a display synthesis procedure which utilizes the control theoretic or optimal pilot model (ref. 7). The particular display design problem to be addressed concerns synthesizing a format for a head-down, stroke-written, CRT display for use in the NASA V/STOLAND integrated digital avionics system, as adapted for use in a UH-1H helicopter. A portion of the landing approach task for the UH-1H vehicle will be utilized in a design example.

V/STOLAND

The NASA Ames Research Center has instituted a vertical takeoff and landing (VTOL) operating experiments program designed to develop a data base for use in establishing system concepts, design criteria, and operational procedures for VTOL aircraft. This technology base will aid in the development of efficient, economical, VTOL short-haul operations with minimum adverse environmental impact.

As a first step in this process, an experimental avionics hardware/software system, designated V/STOLAND, is being developed for terminal area navigation, guidance, control, and display research for VTOL aircraft. The system will first be flown on a UH-1H helicopter as an interim flight vehicle, prior to later installation for operational research on the XV-15 Tilt-Rotor aircraft.

The heart of the V/STOLAND avionics system is a pair of digital computers referred to as the Basic and Research computers, each with 16,000 words of memory. The Basic computer contains programs for baseline navigation, control, and display. The Research computer provides an arena for research-oriented navigation, control, and display programs.

Figure 1 shows the pilot's display panel layout in the UH-1H test vehicle. In the baseline mode of operation, the stroke-written CRT, called the

Multifunction Display (MFD), provides moving-map, horizontal situation information. In the research mode, the MFD will be used as an integrated guidance and control display. It is the purpose of the synthesis procedure to be described to provide the display format for use on the MFD in the research mode.

PILOT MODELING

The four sections which follow will concern themselves with a general but brief description of the optimal pilot model and a more detailed discussion of three specific capabilities of the model as utilized in this study. These capabilities relate to: (1) a procedure for determining the manner in which the pilot allocates his attention among various display elements, (2) a method for utilizing the model to obtain flight director laws, and (3) a method for utilizing the model to generate numerical pilot opinion ratings of a vehicle's handling qualities. The last two capabilities entail some novel model applications, and all three are pertinent to the display design procedure which is to follow.

Optimal Pilot Model

A detailed description of the optimal pilot model is beyond the scope of this paper. The reader is instead referred to reference 7 for specifics. The basic hypothesis behind the model can be given as follows: Subject to his inherent limitations, the well-trained, well-motivated pilot behaves in an optimal manner. The pilot's control characteristics can be modeled by the solution of an optimal linear control and estimation problem with certain specifications. As utilized in this study, these specifications can be summarized as follows:

1. Time Delay: A pure time delay is included in each of the pilot's control outputs.

2. Neuromuscular dynamics: Each output neuromuscular system is modeled as a first-order lag, or, equivalently, control rate appears in the quadratic index of performance.

3. Observation and motor noise: Each variable which the pilot observes from his display is assumed to contain pilot-induced additive white noise which scales with the variance of the observed variable. Each control output is assumed to contain pilot-induced additive white noise which scales with the variance of the control.

4. Rate perception: If a variable is displayed explicitly, the pilot also perceives the first derivative of the variable but no higher derivatives. The first derivative of the displayed variable is also noise contaminated.

5. Index of performance: The index of performance for the optimization procedure is chosen subjectively by the analyst to mirror what he believes to be the task and control objectives as perceived by the pilot.

The placement of the pilot time delay at the control output constitutes the only major deviation from the model of Kleinman et al. (ref. 7). Here, the delay is represented by a Pade' approximation and is treated as part of the plant dynamics. The model of reference 7 subsumes the delay into the observation process. The only advantage which the Pade' approximation affords is that it allows direct use of existing computational algorithms for the solution of optimal estimation and control problems.

In what follows, a "displayed" variable will refer to a variable explicitly displayed to the pilot by the position of a display indicator. A "perceived" variable will refer to the time rate of change of a displayed variable. An "observed" variable will refer to either a displayed or perceived variable.

Figure 2 is a block diagram of the pilot-vehicle system. The equations which define the optimal pilot model follow.

System state equations-

$$\left.\begin{aligned} \dot{\underline{x}}(t) &= \underline{A}\underline{x}(t) + \underline{B}\underline{u}(t) + \underline{\Gamma}\underline{w}(t) \\ E[\underline{w}(t)\underline{w}^T(t+\sigma)] &= \underline{F}\delta(\sigma) \end{aligned}\right\} \tag{1}$$

where $\underline{x}(t)$ represents the state, $\underline{u}(t)$ represents the pilot's control output before his time delay and neuromuscular dynamics are encountered (see fig. 2), and $\underline{w}(t)$ represents white noise disturbances to be described. These equations include:

(1) the vehicle dynamics,

(2) the turbulence, represented by white noise with unity covariance passed through an appropriate shaping filter,

(3) the pilot's effective time delay, modeled as a first-order Pade' approximation

$$e^{-\gamma s} \doteq \frac{-(s - 2/\tau)}{(s + 2/\tau)} \tag{2}$$

(4) the pilot's neuromuscular dynamics, modeled as a first-order lag

$$G(s) = \frac{1}{T_N s + 1} \tag{3}$$

This lag is dynamically equivalent to including a weighting on control rate in the index of performance and adjusting the weighting coefficient on this term to yield a predetermined value of T_N (ref. 7). In this study, the control rate term is not included in the index of performance.

(5) the motor noise $\underline{v}_m(t)$ which is white in nature with covariance

$$E[\underline{v}_m(t)\underline{v}_m{}^T(t+\sigma)] = \rho'\pi E[\underline{u}(t)\underline{u}^T(t+\sigma)]\delta(\sigma) \tag{4}$$

where ρ' is the predetermined noise signal ratio for the motor noise.

Observation equations-

$$\left.\begin{aligned} \underline{z}(t) &= \underline{Hx}(t) + \underline{v}(t) = \underline{z}'(t) + \underline{v}(t) \\ E[\underline{v}(t)\underline{v}^T(t+\sigma)] &= \underline{G}\delta(\sigma) \end{aligned}\right\} \tag{5}$$

where $\underline{Hx}(t)$ represents the vector of observed variables, and $\underline{v}(t)$ is the vector of observation noises. The covariances of the individual observation noises are

$$E[v_j(t)v_j(t+\sigma)] = \frac{\rho_j\pi E[z_j'(t)z_j'(t+\sigma)]\delta(\sigma)}{\hat{f}^2(z_j')} \tag{6}$$

where ρ_j is the noise signal ratio associated with the jth observed variable, and $f(z_j')$ is the amplitude-dependent, pure-gain describing function for a threshold-type nonlinearity associated with the jth observed variable (ref. 8). This nonlinearity models pilot indifference thresholds on observed variables.

Just as in reference 5, the effects of task interference can be modeled as an increase in the nominal noise signal ratios for each displayed variable and its observed derivative. Thus,

$$\rho_k = \rho \cdot \frac{1}{f_c} \cdot \frac{1}{f_s} \cdot \frac{1}{f_k} \tag{7}$$

where

ρ = noise signal ratio associated with "full attention" to a display indicator,

f_c = fraction of attention devoted to the control task as a whole,

f_s = fraction of attention devoted to subtask s, for example, longitudinal control,

f_k = fraction of attention devoted to the kth displayed quantity and its perceived derivative in subtask s, for example, control of pitch attitude in the longitudinal subtask.

No task interference is assumed to occur between displayed and perceived variables, only between displayed variables (ref. 9). Thus, a displayed quantity and its perceived time derivative have the same f_k and ρ_k. Given values of f_c and f_s, it is assumed that the pilot allocates his attention (selects

the f_k) so as to minimize the index of performance for the optimization procedure, subject to the constant

$$\sum_{k=1}^{m} f_k = 1.0 , \quad f_k > 0 , \quad k = 1, 2, \ldots, m \tag{8}$$

where m is the number of displayed quantities.

Index of performance-

$$J = E\left\{ \lim_{T\to\infty} \frac{1}{T} \int_0^T [\underline{y}^T(t)\underline{Q}\underline{y}(t) + \underline{u}^T(t)\underline{R}\underline{u}(t)]dt \right\} \tag{9}$$

where

$$\underline{y}(t) = \underline{C}\underline{x}(t) \tag{10}$$

and $\underline{u}(t)$ is the pilot's output before his effective time delay and neuromuscular dynamics are encountered.

Allocation of Attention

Curry et al. (ref. 10) have offered an efficient iterative procedure for determining the fractions of attention f_k which minimize the index of performance (9), subject to the constraint of equation (8). A description of the iterative procedure, as used in this study, follows. After the f_k's are assigned initial values, for example, $f_k = 1/m$, $k = 1, 2, \ldots, m$, the pilot is modeled. After the modeling is complete, a new set of fractions of attention are calculated, and the pilot is modeled again. This procedure continues until the optimum values of f_k are found. In each iteration, the new fractions of attention are found from

$$f_{k_{new}} = f_k - \alpha[(\underline{\nabla}J)_{proj} \cdot \underline{n}_k] \tag{11}$$

where

$f_{k_{new}}$ = the new kth fraction of attention,

α = a constant,

$\underline{\nabla}J = \sum_{k=1}^{m} \frac{\partial J}{\partial f_k} \underline{n}_k$, the gradient of the index of performance J with respect to f_k, expressed in the f_k coordinate system with orthogonal unit vectors $\underline{n}_k$,

$(\underline{\nabla}J)_{proj}$ = the projection of $\underline{\nabla}J$ onto the hyperplane defined by

$$\sum_{k=1}^{m} f_k = 1.0, \text{ and}$$

$(\underline{\nabla}J)_{proj} \cdot \underline{n}_k$ = the inner or dot product of $(\underline{\nabla}J)_{proj}$ and $\underline{n}_k$, that is, the component of $(\underline{\nabla}J)_{proj}$ in the f_k direction.

Assuming that a suitable value of α has been determined, $f_{k_{new}}$ can be found once $\partial J/\partial f_k$ is known. One can show that

$$\frac{\partial J}{\partial f_k} = TR\left[\underline{R}^{1/2}\underline{L}\,\frac{\partial \underline{P}}{\partial f_k}\,\underline{L}^T(\underline{R}^{1/2})^T\right], \quad k = 1, 2, \ldots, m \tag{12}$$

where $\underline{L} = \underline{R}^{-1}\underline{B}^T\underline{S}$, and $\underline{S}$ is the solution to the steady-state control matrix Riccati equation of the pilot modeling problem,

$$-\underline{S}\underline{A} - \underline{A}^T\underline{S} - \underline{C}^T\underline{Q}\underline{C} + \underline{S}\underline{B}\underline{R}^{-1}\underline{B}^T\underline{S} = 0 \tag{13}$$

and $\underline{P}$ is the solution to the steady-state filter matrix Riccati equation of the pilot modeling problem. One can show that $\partial\underline{P}/\partial f_k$ satisfies

$$(\underline{A} - \underline{P}\underline{H}^T\underline{G}^{-1}\underline{H})\,\frac{\partial \underline{P}}{\partial f_k} + \frac{\partial \underline{P}}{\partial f_k}\,(\underline{A}^T - \underline{H}^T\underline{G}^{-1}\underline{H}\underline{P}) - \underline{P}\underline{H}^T\,\frac{\partial \underline{G}^{-1}}{\partial f_k}\,\underline{H}\underline{P} = 0, \quad k = 1, 2, \ldots, m \tag{14}$$

Now, with

$$\frac{\partial \underline{G}^{-1}}{\partial f_k} \doteq \frac{1}{f_k} \cdot \frac{1}{g_{ii}}, \quad k = 1, 2, \ldots, m \tag{15}$$

where g_{ii} is the diagonal element of $\underline{G}$ corresponding to the kth displayed variable and its perceived derivative, equation (14) can be solved for $\partial\underline{P}/\partial f_k$. Then, equation (12) will yield the value for $\partial J/\partial f_k$ which can be used in equation (11) to find $f_{k_{new}}$.

The author has found that no more than four iterations are usually necessary to find reasonably accurate representations of the optimum f_k. Although the constant α can be changed in each iteration (ref. 11), it was found that setting $\alpha = 50.0$ led to satisfactory convergence for the problems considered here.

Flight Director Design

A flight director system is one in which the various displayed and/or sensed variables used by the pilot in performing a given task are combined into one instrument, forming a single-loop compensatory tracking task for each

of the controls available to the pilot. The flight director and the "laws" which govern the movement of the display elements which constitute the director, can significantly reduce the pilot's workload. In certain situations, such as V/STOL approach and landing tasks, a well-designed director can be a necessity.

The flight director design problem obviously centers about determining the director laws, that is, finding the appropriate mix of vehicle motion quantities to drive the director display elements. As pointed out in reference 12, this mix has historically been determined (1) by adapting and displaying the output of an automatic flight control system, or (2) by choosing appropriate vehicle motion quantities based upon guidance and control requirements. Neither of these approaches explicitly considers the pilot-centered characteristics until the system is simulated or flight tested. The work of reference 12 considers the use of classical frequency-domain representations of the human pilot in director design problems. A director design procedure using the optimal pilot model is suggested in reference 13. Both techniques offer considerable improvement over design procedures (1) and (2) since pilot characteristics are considered at the design stage.

In the research to be described, a simplified director design technique using the optimal pilot model is utilized in which only essential feedbacks are used in the director laws. Experimental verification of a director designed using this technique can be found in reference 14. The technique can be summarized as follows:

(1) Given the vehicle/turbulence model and the baseline display, generate an optimal pilot model. The pertinent results of this analysis will be: (a) predicted pilot transfer functions $h_{ij}(s)$ between each optimal control output $u_i(t)$ and each observed variable $z_j'(t)$, and (b) the average power P_{ij} in each optimal control output $u_i(t)$ which is associated with each observed variable $z_j'(t)$.

(2) Order each pilot transfer function $h_{ij}(s)$ calculated in step (1a) according to the magnitude of the corresponding P_{ij} calculated in step (1b). Based upon this order, choose n_e "essential" observed variables for each control $u_i(t)$.

(3) Formulate the flight director laws (one for each control) as follows:

$$d_i(s) = \sum_{j=1}^{n_e} h_{ij}(s) z_j'(s) \tag{16}$$

(4) Since the a priori assumptions implicit in formulating the pilot model in step (1) may be in error, use simulation results to refine the model. With the refined model, repeat steps (1) through (3) and simulate again.

The method summarized here differs from that offered in reference 13 in two ways: only "essential" variables are utilized in the director laws, and

the subject's neuromuscular dynamics are not included in the transfer functions used to describe the director laws.

The simplifications inherent in considering only the essential variables in the director design are obvious. The exclusion of the subject's neuromuscular dynamics is consistent with the structure of the optimal pilot model. Specifically, the subject's physiological control-rate limitations are dynamically represented by a task-invariant, first-order lag. Including the lag in the director law would be redundant, since the subject himself will generate the lag, regardless of the form of the display compensation.

Pilot Opinion Ratings

A method for generating numerical pilot opinion ratings using the optimal pilot model has been offered in reference 15. The method is contained in a rating hypothesis which states that the numerical rating which a human pilot assigns to a specific vehicle and task can be directly related to the numerical value of the index of performance resulting from the optimal pilot modeling procedure as applied to that vehicle and task. The hypothesis was tested in reference 15 using the data from four piloted simulations and was shown to be reasonable. The pilot rating hypothesis can be stated as follows:

IF (1) the index of performance and model parameters in the optimal pilot modeling procedure yield a dynamically representative model of the human pilot, (2) the variables selected for inclusion in the index of performance are directly observable by the pilot, (3) the weighting coefficients in the index of performance are chosen as the squares of the reciprocals of maximum "allowable" deviations of the respective variables, and these deviations are consonant with the task as perceived by the pilot, THEN the numerical value of the index of performance resulting from the modeling procedure can be related to the numerical pilot rating which the pilot assigns to the vehicle and task by

$$R = R(J)_s$$

where $R(J)_s$ represents a monotonic function of the value of the index of performance J. The subscript s denotes the particular rating scale being utilized by the pilot.

Implicit in the hypothesis is the assumption that once the function $R(J)_s$ has been found for a specific scale s, it can be utilized to assign pilot ratings to any vehicle and task, provided, of course, that the assumptions (1)-(3) are met.

Figure 3 shows the rating function $R(J)_s$ obtained in reference 15 for the Cooper-Harper rating scale of figure 4. The function was shown to yield very acceptable predictions of the actual pilot ratings obtained in single-axis simulations. It should be noted that the rating hypothesis is not limited to single-axis tasks. For example, pilot ratings for longitudinal and lateral aircraft control tasks can be generated from

$$R = R(J_{long} + J_{lat})_s$$

where J_{long} and J_{lat} represent values of the index of performance obtained in modeling the pilot in the longitudinal and lateral tasks, respectively. However, no experimental validation of the multi-axis capability of the rating hypothesis has been undertaken to date.

The potential of the rating hypothesis is eroded somewhat by the lack of a well-defined procedure for selecting pilot model parameters a priori, given a specific vehicle and task, and by difficulty in identifying these pilot model parameters a posteriori, given simulation data (ref. 16). One can, however, suggest a reasonable procedure for selecting the parameters which minimizes the guesswork involved in applying the optimal pilot model. This procedure consists of a group of somewhat conservative rules of thumb for applying the model to problems of <u>design</u> such as the display synthesis which is the subject of the research to be described. As outlined in reference 15, the modeling procedure goes as follows:

(1) Select τ, T_N, ρ, and ρ' as

$$\tau = T_N = 0.2 \text{ sec}$$

$$\rho = \rho' = 0.01$$

(2) Select the maximum allowable deviations of each observed variable in the index of performance as that deviation producing a display indicator movement which subtends a specific visual arc or arc rate at the pilot's eye. Values of 0.5°-1.0° and 0.5°-1.0°/sec appear to be reasonable. For the control movement, select the maximum allowable deviation as a specific percentage of the maximum control motion possible, 25 percent being a reasonable figure.

(3) Select the indifference thresholds on each observed variable to be a specific percentage of the visual arc and arc rate selected in rule (2). Here again, 25 percent would be a reasonable value. Do not allow these threshold values to be smaller than the thresholds associated with visual discrimination, that is, 0.05° and 0.05°/sec.

(4) Use the model for task interference to select the fraction of attention for each displayed variable. This means that in equation (7), f_k values are chosen to minimize the index of performance and satisfy the constraint of equation (8). In equation (7), select

$f_c = 0.5$, that is, assume one-half of the pilot's attention is devoted to control activity as opposed to noncontrol activity, such as monitoring powerplant status, etc.

$f_s = 1/n$, where n is the number of independent modes, for example, longitudinal and lateral ($n = 2$). If multi-axis ratings are to be generated, find the f_s which minimizes the index of performance subject to the constraint

$$\sum_{s=1}^{n} f_s = 1.0 , \quad f_s > 0 , \quad s = 1, 2, \ldots, n.$$

This selection of the optimum f_s fractions can be quickly accomplished by first finding the optimum fractions f_k with $f_s = 1/n$, then initiating a direct search for the optimum f_s fractions while holding the f_k fractions constant. The f_k fractions are usually a very weak function of the f_s fractions, so no further iteration on the f_k fractions are necessary once the optimum values for f_s are found.

(5) Use the rating scheme to predict general flying qualities levels rather than specific numerical ratings. These levels are: Level 1 - A1 to A3.5, Level 2 - A3.5 to A6.5, Level 3 - A6.5 to U9.0$^+$.

The rating hypothesis and modeling procedure outlined above will be utilized in the multi-axis display synthesis to be described.

DESIGN PROCEDURE

The procedure to be outlined is offered as a relatively straightforward, nearly algorithmic method for deriving and then utilizing model-based, pilot-centered requirements in the design of displays for aircraft being flown under IMC. As will be seen, it is hypothesized that if one follows the rational, albeit somewhat dogmatic, design steps, an acceptable display format will be obtained for the vehicle and task at hand. With the present state of the art, the uncertainties inherent in modeling the human in a multiloop, multi-axis control task preclude a more definitive design methodology. It is felt, however, that the design procedure can provide a rational means for generating candidate display formats (including flight director laws) for simulator evaluation.

The optimal pilot model forms the backbone of the design procedure. The model has been experimentally validated in a variety of single-axis manual control studies, and recently has been exercised in a multi-axis analysis of an existing cockpit display in the NASA augmentor wing research aircraft (ref. 5).

The displays referred to in the design procedure concern visual stimuli only. Displays which are directed toward other sensory modalities, for example, tactile displays, will not be treated. In addition, the design procedure is directed specifically toward synthesizing formats for head-down electronic displays, although the general philosophy should be amenable to the design of head-up formats.

In what follows, the design method will first be outlined and discussed. The procedure will then be applied to the problem of defining a candidate display format for the UH-1H V/STOLAND Multifunction Display in a 40-knot landing approach flight path segment.

Specifics

The display design procedure can be given as follows:

(1) Specify the vehicle, environment (winds, turbulence), and task. This includes:

(a) nominal flight path for completion of the task. This also means specifying command variables such as airspeed, etc., along the path;

(b) vehicle dynamics and disturbances linearized about the nominal flight path which may have to be segmented to accommodate the linearization;

(c) system variables which can be measured and displayed to the pilot along the flight path. These variables include guidance and navigation information, powerplant status information, aircraft states, etc.

(2) Assume that a compensatory display structure will be utilized. Such a first-stage compensatory system provides both minimum requirements and initial points of departure for improvements.

(3) Apply steps (4)-(20) for each segment of the flight path about which linearized dynamics have been obtained.

(4) Define "maximum allowable" deviations of all pertinent system variables. Here, "pertinent" refers to those variables which can be displayed to or perceived by the pilot as compensatory variables.

(5) Determine whether noncontrol information such as powerplant status is vital for the flight path segment under consideration.

(6) Define successful subtask completion in terms of the probability of exceeding the maximum allowable deviations of a subset of the variables specified in step (1c).

(7) Define a ficticious cockpit display (virtual display) in which all the variables of step (4) are displayed. This display is merely a list of variables and display gains to be used in the pilot modeling procedure. Select the display gains so that the maximum allowable deviations of step (4) subtend 0.5° or 0.5°/sec (if rates are displayed) of visual arc at the pilot's eye. If the maximum allowable deviations of a displayed variable and its perceived derivative differ, use the deviation of the displayed variable in selecting the display gain.

(8) Model the pilot using the optimal pilot model, the vehicle and disturbances of step (1), and the virtual display of step (7). Select the model parameters as outlined in the preceding discussion on generating pilot ratings.

(9) Determine the optimal allocation of attention between modes.

(10) Obtain the following from the modeling procedure for each mode, for example, longitudinal and lateral:

(a) root-mean-square performance (deviations from nominal flight path),

(b) pilot transfer functions,

(c) relative average power in each control associated with each observed variable,

(d) allocation of attention for each display indicator,

(e) the scalar quantity(s) related to the probability of successful subtask completion,

(f) the predicted handling qualities level.

(11) Modify, if necessary, the appropriate maximum allowable deviations (including virtual display gains, thresholds, and index of performance coefficients) if rms displayed variable predictions are within the selected indifference thresholds or approaching the 0.5°, 0.5°/sec visual arc maximums.

(12) Reduce, if possible, the number of displayed variables if a particular variable and its perceived derivative have associated with it:

(a) a low fraction of attention, for example, less than 10 percent,

(b) a low normalized average power, for example, less than 10 percent, obtained by dividing the power associated with each observed variable by the largest power for each control.

(13) Repeat, if necessary, steps (7)-(12) with the modified display until the modeling procedure yields little changes from iteration to iteration.

(14) Determine whether the inclusion (or modification) of a stability augmentation system is needed, based upon the probability of successful subtask completion and predicted handling qualities levels. If no augmentation design or modification is necessary, go to step (17).

(15) Design a suitable stability augmentation system, if necessary, using whatever means at one's disposal.

(16) Repeat steps (8) through (10) with the augmented vehicle.

(17) Design a flight director using the technique described previously.

(18) Tabulate the following information, which has accrued through the design thus far:

(a) a list of variables which need to be displayed to the pilot in compensatory fashion, with suggested display gains,

(b) a measure of the extent to which the perceived derivative of each displayed variable will be utilized by the pilot (obtained from normalized average power calculations and an examination of pilot transfer functions),

(c) allocation of attention results,

(d) suggested flight director laws,

(e) probability of successful subtask completion and handling qualities level,

(f) predicted rms performance,

(g) importance of noncontrol information.

(19) Implement the following display design guidelines:

(a) compensatory display elements:

(i) Locate centrally those displayed variables which have large predicted fractions of attention and normalized average power.

(ii) Locate peripherally those displayed variables which have small fractions of attention and normalized average power.

(iii) Ensure that the display symbology for those variables whose perceived time derivatives contribute significantly to control motion will allow the derivatives to be determined easily by the pilot.

(iv) Locate the flight director symbols as closely as possible to the displayed variables of (i) above, centrally, if possible.

(b) noncontrol information: Noncontrol information, if pertinent, should be located peripherally, but with considerable "peripheral appeal."

(c) pursuit-precognitive display elements: Guidance and navigation information should be provided in a manner which minimizes pilot mental workload in utilizing this information for control purposes, that is, allows pursuit and precognitive behavior on

the part of the pilot. This information can be located peripherally.

(d) control-display relationships: Consistent control-display relationships should be utilized in the design, for example, all "fly-to" symbology.

(20) Analyze the effect of display/vehicle modifications using the optimal pilot model. For example,

(a) the performance variations which accompany different fractions of attention f_c on control, as opposed to monitoring, can be ascertained;

(b) the performance improvement to be expected with the flight director as opposed to the baseline display can be determined.

Discussion

Figure 5 is a flow chart representation of the design process outlined in the preceding section. Although the process appears rather involved, the rationale behind the procedure revolves around the answers to the following five questions:

Given the vehicle, task and environment,

(1) What variables are available for display to the pilot (steps (1)-(7))?

(2) Of the variables in (1), which are essential (steps (8)-(13))?

(3) From the standpoint of pilot/vehicle performance and handling qualities, is display of only the essential variables sufficient, or is some form of stability augmentation desirable (steps (14)-(16))?

(4) How should a flight director be designed (step (17))?

(5) How should the display symbology be arranged (steps (18)-(19))?

Other questions are answered in step (20), for example, Is the inclusion of a flight director worthwhile from the standpoint of predicted improvements in performance and handling qualities?

The introduction of the optimal pilot model to the design procedure is actually begun in step (4) where the concept of "maximum allowable deviations" is introduced. These deviations play a central role in the procedure where they are used to select the display gains on the virtual display, select the pilot indifference thresholds, and select the weighting coefficients in the model index of performance.

The assumption that such maximum allowable deviations exist in the mind of the well-trained pilot is certainly reasonable. For example, the

definition of the Category II landing approach "window" is based upon maximum allowable deviations from a nominal approach condition (ref. 17). Adjusting the display gains so that each maximum deviation subtends the same visual arc or arc rate at the pilot's eye is desirable, that is, the pilot senses that all pertinent displayed variables have the same sensitivity. Finally, the successful use of these maximum deviations in the optimal pilot modeling procedure is well documented, for example, reference 5.

It should be noted that no changes in the maximum allowable deviations or number of displayed variables are considered after the stability augmentation system has been designed. To do so might seriously degrade the performance of the pilot/vehicle system in the event of an augmentation failure.

Questions regarding the selection of the maximum allowable deviations and the application of other elements of the design procedure are probably best answered by the design example of the next section.

EXAMPLE: DISPLAY DESIGN FOR UH-1H LANDING APPROACH

The UH-1H helicopter is a single-engine, single-rotor, light utility helicopter with a mass of approximately 3856 kg in the flight condition studied here. It is desired to synthesize a display for the V/STOLAND MFD for a constant velocity portion of a conventional landing approach task at -6° glide slope. Both longitudinal and lateral motions are to be considered. The vehicle has no stability augmentation system but does possess a stabilizer bar, a device attached to the rotor hub which provides pitch and roll damping. The controls available to the pilot consist of longitudinal and lateral cyclic pitch via a center stick, collective pitch via a side-mounted stick, and tail rotor collective pitch via rudder pedals. No throttle input is required, since rotor rpm is held constant through the action of a power governor.

Design

Step (1)- A -6° glide slope, conventional landing approach task is being considered. A path segment with a constant groundspeed command of 20.6 m/sec (40 knots) is of interest. Table I shows the stability derivatives of the UH-1H vehicle linearized about a level flight condition. The changes in the equations of motion and derivatives for the -6° glide slope are negligible for the purposes of this study. As reference 18 points out, the use of level-flight stability derivatives will lead to slightly conservative predictions of flight path control and workload. The notation and definitions of the derivatives themselves are quite standard (ref. 19).

Table II shows the turbulence spectra used in the study. The spectra are neither von Karman nor Dryden but a simplified form offered in reference 20. The turbulence intensities and characteristic lengths were obtained from reference 21 for the flight phase utilized here (Flight Phase Category C). The system variables which can be measured or calculated by the V/STOLAND system and displayed to the pilot on the flight path segment of interest are

shown in table III. It should be noted that the differentiated variables ($\dot{u}$, etc.) are perceived and not measured or displayed explicitly.

Steps (2)-(4)- The V/STOLAND Multifunction Display has been chosen for study. The display is approximately 76.2 cm from the pilot's eye, and the display area measures 17.5 cm vertically and 16.6 cm horizontally.

The maximum allowable deviations of the compensatory displayed and perceived variables are shown in table III. The maximum values of u, h, and y were directly related to the task of hand, that is, they were based upon the dimensions of the Category II approach window to be described. The maximum deviations of the remaining displayed variables were selected on the basis of the scaling of typical electromechanical instrumentation.

On a typical electromechanical artificial horizon, with an eye-to-display distance of 76.2 cm, 0.5° of subtended visual arc corresponds to 5.0° of displayed pitch attitude. The same holds true for a typical sideslip indicator, where 0.5° of visual arc corresponds to 5.0° of displayed sideslip. Thus, the maximum allowable deviations of θ, ϕ, σ, γ, and ψ were chosen as 5.0° (0.0873 rad). The maximum allowable deviations of the control deflections (measured at the pilot's hands and feet) represent 25 percent of the maximum possible deflection of the pilot's controls as measured in a UH-1H cockpit.

With the exception of $\dot{y}$, the maximum allowable deviations of the perceived variables (derivatives) were chosen to be numerically equal to the maximum allowable deviations of the displayed variables. Since the maximum y was based upon one-half of an average runway width (via the Category II window lateral dimension), it was felt that the maximum $\dot{y}$ should be more conservative and chosen on more dynamic considerations. Hence, the maximum allowable deviation of $\dot{y}$ was made equal to that of $\dot{h}$.

Step (5)- On the basis of pilot eye-point-of-regard measurements, reference 22 shows that an average of 7 percent of the total time spent in performing a 60-knot Instrument Flight Rule (IFR) descent in a UH-1B helicopter was spent fixating the dual tachometer (engine and rotor rpm) and the torquemeter (torque pressure in psi, indicative of torque applied to the engine output shaft). The average percentage fixation time for these two instruments reaches 13 percent in an IFR hover, in ground effect. Although the vehicle and task of reference 22 do not precisely match those of this study, the importance of the dual tachometer and torquemeter to the pilot of a single-engine helicopter in an instrument landing is obvious. This information will be considered vital in this study.

Step (6)- Successful subtask completion will be defined here as remaining inside the Category II approach window dimensions (ref. 17) at all times in the approach segment under study. Although the Category II window was designed to aid the pilots of conventional fixed-wing aircraft in landing approach, its use here is not unreasonable in view of the task similarities. Remaining within the window dimensions means groundspeed deviations of less than 2.57 m/sec (5 knots) in magnitude, glide-slope deviations of less than 3.66 m (12 ft) in magnitude, and course errors of less than 21.9 m (72 ft) in magnitude. Note that these dimensions correspond to the maximum allowable

deviations of u, h, and y, respectively. Due to the stationary statistical nature of the modeling procedure, the introduction of the minimum decision altitude, normally associated with the Category II window, is somewhat artificial in this analysis.

Step (7)- The variables and display gains which define the virtual display are shown in table III.

Steps (8)-(13)- Steps (8)-(13) deal with application of the optimal pilot model. Rather than a detailed description of each of these steps, just the results will be presented here. Table IV lists the definitions of the model indices of performance for the longitudinal and lateral modes. The inclusion of the variables u and h in J_{long} and y in J_{lat} are obvious choices in view of the nature of the task. The inclusion of $\dot{\theta}$ and $\dot{h}$ in J_{long} and $\dot{\psi}$, $\dot{\phi}$, and $\dot{y}$ in J_{lat} are based upon the subjective estimate that large angular or linear velocity perturbations would be unacceptable to the pilot.

In applying step (11) for the lateral case, it was found that the maximum allowable deviations in roll angle ϕ and course error y had to be reduced in order to bring the rms values of these displayed variables out of the thresholds. Acceptable maximum allowable deviations of ϕ and y were determined to be 0.0542 rad and 17.5 m, respectively. The maximum allowable deviations of $\dot{\phi}$ and $\dot{y}$ were not altered. The new virtual display gains were calculated as 12.3 cm/rad for ϕ, 12.3 (cm/sec)/(rad/sec) for $\dot{\phi}$, 0.0381 cm/m for y, and 0.0381 (cm/sec)/(rad/sec) for $\dot{y}$.

Figure 6 (Baseline) shows the value of the model index of performance vs the fraction of attention on the longitudinal (or lateral) task. From this it can be seen that a 50-50 allocation of attention between lateral and longitudinal modes is optimum. Also shown in figure 6 is the Cooper-Harper pilot rating associated with the minimum value of J. This A5.9 value was found from figure 3 and represents Level 2 handling qualities.

The first data column of table V (Baseline) shows the predicted rms performance values along with the probability of remaining within the Category II window. Figure 7 shows the normalized average power in each control due to the observed variables indicated above the bars. These power values were obtained by normalizing the power for each control and variable by the largest power for each control. Also shown are the fractions of attention on the observed variables. Table VI lists the simplified forms of the pilot transfer functions obtained from the modeling procedure. These relate the pilot's control motions to the vehicle motion variables. These transfer functions were obtained by eyeball fit of straight-line asymptotes to the frequency response diagrams obtained from the modeling procedure. Although the actual transfer functions are calculated as part of the model output, they are of unacceptably high order for the purposes of designing flight directors. These actual transfer functions can, however, be very adequately represented by lower order approximations (ref. 13).

Steps (14)-(16)- On the basis of the predicted Level 2 handling qualities for the Baseline pilot/vehicle system, some type of stability augmentation system appears warranted. The following definition for Level 2 handling

qualities is taken from Section 1.5 of reference 23, where the landing approach task falls into Flight Phase Category C:

> Level 2: Flying qualities adequate to accomplish the mission Flight Phase, but some increase in pilot workload or degradation in mission effectiveness, or both, exists.

In terms of the task defined here, longitudinal control is more "difficult" than lateral. The longitudinal task alone has a predicted pilot rating of A4.6 ($J_{long} = 0.43$) as compared to the lateral rating of A1 ($J_{lat} = 0.15$). Also, as figure 6 indicates, longitudinal performance degrades more rapidly than lateral for off-nominal fractions of attention f_s.

The 0.021 probability of not remaining in the Category II window (see table V) is due almost entirely to violating the longitudinal window dimensions, that is, groundspeed and glide-slope excursions. The probability of violating the lateral window dimensions is negligible.

It should be noted that some augmentation of the lateral mode may be desirable. Although predicted handling qualities appear very acceptable, figure 7 indicates that a good deal of perceived heading rate ($\dot{\psi}$) is used in driving the pedals. While such heading control may not be difficult, the demands it makes upon the pilot's attention could be alleviated by yaw rate feedback to the tail rotor. For the purposes of this study, however, only longitudinal stability augmentation is considered.

Perhaps the simplest longitudinal stability augmentation design would involve implementing a "groundspeed-hold" system, thus relieving the pilot of that task. As figure 7 shows, groundspeed accounts for the dominant portion of longitudinal cyclic power, and the groundspeed display has a 0.22 fraction of attention associated with it.

Based upon the Bode-gain of the simplified dominant pilot transfer function, $\delta_E(s)/u(s)$, a longitudinal cyclic stability augmentation command (applied in parallel with the pilot's input) was created:

$$\delta_{E_a}(t) = -0.00404u(t) \text{ meters}$$

Figure 6 (Stab-Aug) shows the value of the model index of performance vs the fraction of attention on the longitudinal task for the pilot/vehicle system with stability augmentation. Again, it can be seen that a 50-50 allocation of attention between lateral and longitudinal modes is optimum. The Cooper-Harper pilot rating and corresponding handling qualities level are also shown.

The second data column of table V (Stab-Aug) shows the predicted rms performance values along with the probability of remaining within the Category II window for the augmented pilot/vehicle system. Figure 8 shows the normalized average power in each control due to the observed variables indicated above the bars. Also shown are the fractions of attention on the observed variables. Finally, table VI lists the simplified forms of the pilot transfer functions

between control and motion variables for the augmented system. Since the longitudinal and lateral modes are dynamically uncoupled, and a 50-50 allocation of attention is still optimum, the addition of a longitudinal stability augmentation system effects only the pilot transfer functions associated with longitudinal control.

According to the predicted handling qualities level of figure 6 (Stab-Aug), the vehicle handling qualities still are not satisfactory. This is not too surprising, since the stability augmentation design was quite rudimentary in nature and was intended primarily to emphasize the rationale behind placing stability augmentation design at this point in the analysis. For purposes of exposition, it will be assumed that the stability augmentation is satisfactory, and we will proceed with the flight director design.

Step (17)- Longitudinal and lateral flight director laws were designed using the director design technique outlined previously. According to equation (16), director laws are formulated for each control available to the pilot. It has been pointed out, however, that director systems requiring a compensatory pedal command signal are not considered desirable in light of pilot workload, which increases as the number of director commands increase (ref. 24). Since predicted rms pedal motion is rather small for this study (less than 0.1 cm as shown in table V), it was decided to consider just three director commands: longitudinal cyclic, collective, and lateral cyclic. Such "three-cue" directors have been evaluated in UH-1 flight tests (ref. 25), so the concept is not unreasonable.

When the transfer functions of table VI (Stab-Aug), the normalized average power calculations of figure 8, and equation (16) were applied, the director design technique yielded the following laws:

(1) longitudinal cyclic,

$$d_1 = \frac{1}{(s + 0.35)(s + 0.3)} (-0.00380h - 0.168\gamma) \text{ meters}$$

(2) collective,

$$d_2 = \frac{1}{(s + 0.7)} (-0.00620h - 0.296\gamma) \text{ meters}$$

(3) lateral cyclic,

$$d_3 = \frac{1}{(s + 0.8)^2} [-0.149(s + 0.15)\sigma - 0.0328s\psi - 0.000195(s + 0.25)y] \text{ meters}$$

In these equations, h, γ, σ, ψ, and y are expressed in terms of vehicle motion rather than in display indicator movement.

Steps (18)-(19)- The information called for in step (18) has already been tabulated in the previous steps. Figure 9 illustrates a candidate display

format which has been designed via the guidelines of step (19). In what follows, the term "central" will refer to the center of the aircraft, symbol (18), which serves as a null point for the compensatory elements (6), (7), (8), and (21) in the figure.

(a) compensatory display elements:

(i) According to figure 8, the variables γ, h, σ, ψ, and y have large fractions of attention and normalized average power associated with them. Consequently, the symbols for these variables have been centrally located in the display, that is, γ and σ in the vertical and horizontal translation of symbol (6); h and y in the vertical and horizontal translation of symbol (7); and ψ in the horizontal translation of symbol (8).

(ii) The variables u, θ, and ϕ have smaller fractions of attention and normalized average power associated with them. Consequently, the symbol for u, (19), which extends either above (fast) or below (slow) the aircraft symbol, has been located peripherally. In order to reduce central display clutter, the artificial horizon, symbol (21), has been segmented. The small fractions of attention associated with θ and ϕ allow the artificial horizon to be deemphasized here.

(iii) According to figure 8, the perceived rate of heading error $\dot{\psi}$ dominates pedal activity. The translating bar of symbol (8) should allow easy rate detection by the pilot, that is, the symbol is always in contact with the stationary reference aircraft symbol (18).

(iv) The flight director symbols (3), (4), and (20) have been located as close as possible to the central display elements of (i) above. It would be advantageous, of course, to locate these symbols centrally, particularly the cyclic director bars. Past experiments have shown, however, that such overlapping symbology on the MFD can be confusing to the pilot (ref. 2).

(b) noncontrol information: The dual-tachometer (16) and torquemeter (10) have been located remotely from the central area of the display. The dual-tachometer shows only the rpm range of interest for UH-1H operation, that is, engine rpm from 6000 to 7200 and rotor rpm from 300 to 360. In normal operation, the triangular pointers move synchronously up and down the scale. When a malfunction such as an engine failure occurs, the pointers will separate. Immediate engine failure detection by the pilot is essential in order to establish autorotation, and consequently, such detection constitutes the primary utility of the dual-tachometer. The triangular pointer on the torquemeter moves vertically along the scale which reads from 0 to 50 psi of "torque pressure."

(c) pursuit-precognitive display elements: The moving-map, horizontal situation display elements of figure 9 (symbols (11)-(15)) are designed to relieve the pilot of considerable mental workload in confirming his position and to enable him to adopt higher than compensatory levels of skill (pursuit-precognitive) while negotiating curved courses or making flight path corrections. The triangular aircraft symbol (13) is fixed on the display in "heading-up" fashion. Other display elements which are not a direct result of the design procedure have been included in the format of figure 9. The roll indicator (1) can be used by the pilot to establish turn rates for curvilinear flight paths. The distance-to-go (5), altitude (9), vertical speed (17), and groundspeed (22) digital readouts provide useful status information for the pilot regarding the progress of the landing approach.

Step (20)- It is of interest to use the pilot model in assessing the pilot/vehicle performance to be expected with the flight director which was designed in step (17). To this end, the pilot model was employed in a manner nearly identical to that of step (8). The observed variables and display gains for the director case are shown in table VII. Note that since no pedal director was implemented the pilot was assumed to observe σ, $\dot{\sigma}$, ψ, and $\dot{\psi}$ for pedal control, as per the lateral normalized power predictions of figure 8. The model indices of performance for the director configuration are identical to those of table IV.

In the modeling, the rms values of the director commands were found to be smaller than the indifference thresholds (25 percent of the maximum allowable deviations of table VII). Since the maximum allowable deviations of the director commands do not appear in the model indices of performance, only the director display gains were changed in order to bring the rms values of the director commands out of the thresholds. The new director gains were chosen as: $d_1 \rightarrow 175$ cm/m; $d_2 \rightarrow 43.8$ cm/m; $d_3 \rightarrow 175$ cm/m.

Figure 6 (Stab-Aug and Director) shows the value of the model index of performance vs the fraction of attention on the longitudinal task for the director case with the longitudinal stability augmentation system included. Again a 50-50 allocation of attention is optimum. The Cooper-Harper rating and handling qualities level are also shown. The third data column of table V (Director) shows the predicted rms performance values. Since no pedal director was implemented in the design, the manner in which the pedal motion was generated was of interest. Figure 10 shows the normalized average power in the lateral cyclic and pedals due to each of the observed variables indicated. Also shown are the fractions of attention on the observed variables for lateral control. As the figure indicates, lateral cyclic motion is dominated entirely by the appropriate director command, whereas the lateral cyclic director command and heading rate dominate pedal motion. Note that over 80 percent of the pilot's lateral mode attention is devoted to the cyclic director command. Based upon the general performance improvement evident in table V, the dramatic decrease in predicted handing qualities level, and the very small rms pedal motion, the three-cue flight director design appears quite acceptable.

Discussion

Reference (26) documents an Air Force study in which a representative cross section of currently qualified Air Force helicopter pilots were queried by means of a questionnaire regarding their opinion of the displays and flight control systems of their helicopters. The response data were divided into two general helicopter categories: heavy lift (H/L) and light lift (L/L). Although all responses were analyzed by specific helicopter type, it was determined that differences between vehicle types were generally not as significant as differences between H/L and L/L responses. Of the 77 L/L pilots who responded, 95 percent were pilots of variants of the UH-1 helicopter (UH-1H, UH-1N, etc.). With this high percentage of UH-1 pilots in the L/L category, it is interesting to compare three applicable L/L pilot questionnaire responses regarding the landing approach flight task with some of the more general results of the analytical display design study just completed for the UH-1H vehicle. From reference 26:

(1) The single most requested display improvement was the addition of a helicopter flight director system (81 percent of the L/L pilots). Those pilots with previous flight director experience were more in favor of the director than those without such experience. Lack of basic vehicle stability was presented as rationale by those L/L pilots who favored a flight director and by those who did not. Those in the former category pointed out that director command information might help compensate for lack of stability, while those in the latter category felt their helicopters were so unstable that the stability must be treated before the pilot could use any advanced displays.

(2) When asked to relate the degree of difficulty in controlling various axes during steep landing approaches (glide slope steeper than -3°), it was determined that the pitch axis (airspeed control) was the most difficult, followed by collective control, then yaw axis, with the roll axis rated as the least difficult.

(3) When asked to assess the priority of stability augmentation for steep approaches below 50 knots, yaw axis stability was identified as the first to be installed. The apparent contradiction between this response and that in (2) was explained by the fact that pilot comments indicated that yaw, while not difficult to control, did occupy the pilot to the extent that he felt that it should be the first axis augmented.

Result (1) above tends to corroborate one of the primary findings of this design study, that is, the general desirability of a flight director system. The question of whether stability augmentation should precede flight director implementation is answered in the flow chart of figure 5, where flight director design is considered only after the desirability of stability augmentation has been determined.

Result (2) above supports the conclusion of design step (14), that is, longitudinal control is most difficult.

Result (3) above runs counter to the design study's choice of the pitch axis as the first to be included in a stability augmentation system. The design study did point out, however, that perceived yaw rate $\dot{\psi}$ dominated pedal activity, and that consequently, some form of yaw augmentation may be desirable.

CONCLUSIONS

Based upon the display design procedure and example which have been discussed, the following conclusions can be drawn:

(1) The display design procedure appears to be a useful and reasonably straightforward way of determining model-based, pilot-centered display requirements. The pertinent information obtained from the modeling procedure is:

(a) a list of variables which need to be displayed to the pilot in compensatory fashion with suggested display gains,

(b) a measure of the extent to which the perceived derivative of each displayed variable is utilized by the pilot,

(c) allocation of attention results, between modes and among display indicators in each mode,

(d) suggested flight director laws,

(e) probability of successful subtask completion and handling qualities levels,

(f) rms performance.

(2) The generation of multi-axis pilot opinion ratings (handling qualities levels) using the model-based procedure of reference 15 appears to be feasible. Although no actual pilot opinion rating data were available for comparison, the predicted handling qualities levels were reasonable for this vehicle and task.

(3) The design procedure is, of course, a prelude to simulator evaluation. Since there is no direct constructive procedure to go from the general requirements of (1) above to a specific, unique display format, a number of competing formats can be generated. These can then be evaluated in simulation.

(4) The modeling procedure shows potential for the design of stability augmentation systems.

REFERENCES

1. V/STOL Displays for Approach and Landing. AGARD Rep. No. 594, 1972.

2. Murphy, M. R.; McGee, L. A.; Palmer, E. A.; Paulk, C. H.; and Wempe, T. E.: Simulator Evaluation of Three Situation and Guidance Displays for V/STOL Zero-Zero Landings. Proceedings of the Tenth Annual Conference on Manual Control, April 1974, pp. 439-465.

3. Clement, W. F.; McRuer, D. T.; and Klein, R. H.: Systematic Manual Control Display Design. Proceedings of the 13th AGARD Guidance and Control Symposium on Guidance and Control Displays, AGARD CP-96, 1971, pp. 6-0 to 6-10.

4. Kleinman, D. L.; and Baron, S.: Analytic Evaluation of Display Requirements for Approach to Landing. NASA CR-1952, 1971.

5. Baron, S.; and Levison, W. H.: A Display Evaluation Methodology Applied to Vertical Situation Displays. Proceedings of the Ninth Annual Conference on Manual Control, May 1973, pp. 121-132.

6. Hess, R. A.; and Wheat, L. W.: A Model-Based Analysis of a Display for Helicopter Landing Approach. IEEE Transactions on Systems, Man and Cybernetics, vol. SMC-6, no. 7, 1976, pp. 505-511.

7. Kleinman, D. L.; Baron, S.; and Levison, W. H.: An Optimal Control Model of Human Response, Parts I and II. Automatica, vol. 6, 1970, pp. 357-383.

8. McRuer, D. T.; and Graham, D.: Analysis of Nonlinear Control Systems. John Wiley & Sons, Inc., 1961, pp. 230-244.

9. Levison, W. H.; Elkind, J. I.; and Ward, J. L.: Studies of Multivariable Manual Control Systems: A Model for Task Interference. NASA CR-1746, 1971, p. 13.

10. Curry, R. E.; Kleinman, D. L.; and Hoffman, W. C.: A Model for Simultaneous Monitoring and Control. Proceedings of the Eleventh Annual Conference on Manual Control, May 1975, pp. 144-150.

11. Luenberger, D. G.: Optimization by Vector Space Methods. John Wiley & Sons, Inc., 1969, pp. 283-290.

12. Weir, D. H.; Klein, R. H.; and McRuer, D. T.: Principles for the Design of Advanced Flight Director Systems Based on the Theory of Manual Control Displays. NASA CR-1748, 1971.

13. Levison, W. H.: A Model-Based Technique for the Design of Flight Directors. Proceedings of the Ninth Annual Conference on Manual Control, May 1973, pp. 163-172.

14. Duffy, T. W.: An Analysis of the Effect of a Flight Director on Pilot Performance in a Helicopter Hover Task. M.S. Thesis, Dept. of Aeronautics, Naval Postgraduate School, Monterey, Calif., 1976.

15. Hess, R. A.: A Method for Generating Numerical Pilot Opinion Ratings Using the Optimal Pilot Model. NASA TM X-73,101, 1976.

16. Phatak, A.; Weinert, H.; and Segall, I.: Identification of the Optimal Control Model for the Human Operator. AMRL-TR-74-79, Aerospace Medical Research Laboratory, 1974.

17. Graham, D.; Clement, W. F.; and Hofmann, L. G.: Investigation of Measuring Systems Requirements for Instrument Low Visibility Approach. AFFDL-TR-70-102, Air Force Flight Dynamics Laboratory, 1971, pp. 7-10.

18. Clement, W. F.; and Hofmann, L. G.: A Systems Analysis of Manual Control Techniques and Display Arrangements for Instrument Landing Approaches in Helicopters. Vol. 1. Speed and Height Regulation. Rep. 183-1, Systems Technology, Inc., 1969, pp. A1-A5.

19. McRuer, D. T.; Ashkenas, I.; and Graham, D.: Aircraft Dynamics and Automatic Control. Princeton University Press, 1973, pp. 255-262.

20. Hart, J. E.; Adkins, L. A.; and Lacau, L. L.: Stochastic Disturbance Data for Flight Control System Analysis. ASD-TDR-62-347, Air Force Aeronautical Systems Division, 1962, p. 67.

21. Military Specification - Flying Qualities of Piloted Airplanes. MIL-F-8785B, 1969, pp. 48-52.

22. Barnes, J. A.: Analysis of Pilot's Eye Movements During Helicopter Flight. Tech. Memorandum 11-72, Army Aberdeen Research and Development Center, 1972.

23. Military Specification - Flying Qualities of Piloted V/STOL Aircraft. MIL-F-83300, 1970.

24. Klein, R. H.; and Clement, W. F.: Application of Manual Control Display Theory to the Development of Flight Director Systems for STOL Aircraft. AFFDL-TR-72-152, Air Force Flight Dynamics Laboratory, 1973, p. 61.

25. Santanelli, A.; and Kurkowsky, R.: Evaluation of Three-Cue Flight Director Systems. ECOM-4385, Army Electronics Command, 1976.

26. Clark, W. E.; and Intano, G. P.: Helicopter Display Improvement Study. IFC-TN-75-1, Air Force Instrument Flight Center, 1975.

TABLE I.- NORMALIZED UH-1H STABILITY DERIVATIVES IN STABILITY AXIS SYSTEM

Longitudinal		
$m = 3\ 856$ kg	$Z_w = -0.802$/sec	$X_{\delta_C} = -1.07/sec^2$
$U_o = 20.6$ m/sec (40 knots)	$Z_q = 7.25$ m/sec	$Z_{\delta_E} = 12.5/sec^2$
$I_{yy} = 17\ 261$ kg-m^2	$M_u = 0.00432$/m-sec	$Z_{\delta_C} = -108/sec^2$
$X_u = -0.0257$/sec[a]	$M_w = -0.0248$/m-sec	$M_{\delta_E} = -6.57/m\text{-}sec^2$
$X_w = 0.000423$/sec	$M_q = -2.96$/sec	$M_{\delta_C} = 1.46/m\text{-}sec^2$
$X_q = 5.53$ m/sec	$M_{\dot{w}} = 0$/m	δ_E = longitudinal cyclic motion measured at pilot's hand
$Z_u = -0.120$/sec	$X_{\delta_E} = 10.4/sec^2$	δ_C = collective motion measured at pilot's hand
Lateral		
$I_{xx} = 3797$ kg-m^2	$Y_{\delta_P} = -10.0/sec^2$	$N_p = -0.177$/sec
$I_{zz} = 14\ 644$ kg-m^2	$L_v = -0.057$/m-sec	$N_r = -0.787$/sec
$I_{xz} = 2007$ kg-m^2	$L_p = -12.8$/sec	$N_{\delta_A} = -0.126/m\text{-}sec^2$
$Y_v = -0.0797$/sec	$L_r = 2.12$/sec	$N_{\delta_P} = 23.0/m\text{-}sec^2$
$Y_p = -5.83$ m/sec	$L_{\delta_A} = 22.1/m\text{-}sec^2$	δ_A = lateral cyclic motion measured at pilot's hand
$Y_r = 1.23$ m/sec	$L_{\delta_P} = -8.5/m\text{-}sec^2$	
$Y_{\delta_A} = 10.4/sec^2$	$N_v = 0.0771/m\text{-}sec^2$	δ_P = pedal motion measured at pilot's foot

[a]Force and moment derivatives are normalized with respect to mass and moment of inertia.

TABLE II.- ATMOSPHERIC TURBULENCE SPECTRA

Longitudinal
$\Phi_{w_g w_g}(\omega) = \frac{2\sigma_{w_g}^2 L_{w_g}}{U_0} \frac{1}{1 + (L_{w_g}\omega/U_0)^2}$
$\Phi_{u_g u_g}(\omega) = \frac{2\sigma_{u_g}^2 L_{u_g}}{U_0} \frac{1}{1 + (L_{u_g}\omega/U_0)^2}$
σ_{w_g} = 0.762 m/sec (2.5 ft/sec)
σ_{u_g} = 1.52 m/sec (5.0 ft/sec)
L_{w_g} = 152 m (500 ft)
L_{u_g} = 457 m (1500 ft)
Lateral
$\Phi_{v_g v_g}(\omega) = \frac{2\sigma_{v_g}^2 L_{v_g}}{U_0} \frac{1}{1 + (L_{v_g}\omega/U_0)^2}$
σ_{v_g} = 1.52 m/sec (5.0 ft/sec)
L_{v_g} = 457 m (1500 ft)

TABLE III.- OBSERVED VARIABLES AND DISPLAY GAINS

Definition	Variable	Maximum allowable deviation	Display gain
Longitudinal			
Groundspeed error	u	2.57 m/sec (5 knots)	$0.258 \frac{\text{cm}}{\text{m/sec}}$
	$\dot{u}$	2.57 m/sec^2	$.258 \frac{\text{cm/sec}}{\text{m/sec}^2}$
Glide-slope error	h	3.66 m (12 ft)	.182 cm/m
	$\dot{h}$	3.66 m/sec	$.182 \frac{\text{cm/sec}}{\text{m/sec}}$
Pitch attitude error	θ	.0873 rad	7.62 cm/rad
	$\dot{\theta}$	.0873 rad/sec	$7.62 \frac{\text{cm/sec}}{\text{rad/sec}}$
Longitudinal flight path angle error	γ	.0873 rad	7.62 cm/rad
	$\dot{\gamma}$	.0873 rad/sec	$7.62 \frac{\text{cm/rad}}{\text{rad/sec}}$
Longitudinal cyclic	δ_E	.0381 m (0.125 ft)	not displayed
Collective	δ_C	.0381 m	
Lateral			
Roll angle	ϕ	0.0873 rad	7.62 cm/rad
	$\dot{\phi}$	.0873 rad/sec	$7.62 \frac{\text{cm/sec}}{\text{rad/sec}}$
Heading error	ψ	.0873 rad	7.62 cm/rad
	$\dot{\psi}$	.0873 rad/sec	$7.62 \frac{\text{cm/sec}}{\text{rad/sec}}$
Course error	y	21.9 m (72 ft)	.0303 cm/m
	$\dot{y}$	3.66 m/sec (12 ft/sec)	$.0303 \frac{\text{cm/sec}}{\text{m/sec}}$
Lateral flight path angle error	σ	.0873 rad	7.62 cm/rad
	$\dot{\sigma}$	.0873 rad/sec	$7.62 \frac{\text{cm/sec}}{\text{rad/sec}}$
Lateral cyclic	δ_A	.0381 m (0.125 ft)	not displayed
Pedals	δ_P	.0191 m (0.0625 ft)	

TABLE IV.- MODEL INDICES OF PERFORMANCE

$$J = E\left\{\lim_{T\to\infty} \frac{1}{T} \int_0^T [\underline{y}^T(t)\underline{Q}\underline{y}(t) + \underline{u}^T(t)\underline{R}\underline{u}(t)]dt\right\}$$

Longitudinal: J_{long}	
$y_1 = u$	$q_{11} = (1/2.57)^2$ sec^2/m^2
$y_2 = \dot{\theta}$	$q_{22} = (1/0.0873)^2$ sec^2
$y_3 = h$	$q_{33} = (1/3.66)^2$/m^2
$y_4 = \dot{h}$	$q_{44} = (1/3.66)^2$ sec^2/m^2
u_1 = longitudinal cyclic motion before pilot's time delay and neuromuscular dynamics	$r_{11} = (1/0.0381)^2$/m^2
u_2 = collective motion before pilot's time delay and neuromuscular dynamics	$r_{22} = (1/0.0381)^2$/m^2
Lateral: J_{lat}	
$y_1 = \dot{\psi}$	$q_{11} = (1/0.0873)^2$ sec^2
$y_2 = \dot{\phi}$	$q_{22} = (1/0.0873)^2$ sec^2
$y_3 = y$	$q_{33} = (1/21.9)^2$/m^2
$y_4 = \dot{y}$	$q_{44} = (1/3.66)^2$ sec^2/m^2
u_1 = lateral cyclic motion before pilot's time delay and neuromuscular dynamics	$r_{11} = (1/0.0381)^2$/m^2
u_2 = pedal motion before pilot's time delay and neuromuscular dynamics	$r_{22} = (1/0.0191)^2$/m^2

TABLE V.- ROOT-MEAN-SQUARE PERFORMANCE PREDICTIONS

Variable	Baseline	Stab-Aug	Director
Longitudinal			
σ_u (m/sec)	0.942	0.600	0.622
σ_w (m/sec)	.655	.582	.497
σ_θ (rad)	.0208	.0166	.0165
$\sigma_{\dot{\theta}}$ (rad/sec)	.0103	.00689	.00618
σ_h (m)	1.49	1.34	.777
$\sigma_{\dot{h}}$ (m/sec)	.588	.564	.416
σ_{δ_E} (m)	.00548	.00330	.00289
σ_{δ_C} (m)	.00914	.00914	.00820
Lateral			
σ_v (m/sec)	1.58	same as Baseline	1.58
σ_ϕ (rad)	.0152		.00911
$\sigma_{\dot{\phi}}$ (rad/sec)	.00769		.00514
σ_ψ (rad)	.0802		.0786
$\sigma_{\dot{\psi}}$ (rad/sec)	.0207		.0204
σ_y (m)	4.51		2.72
$\sigma_{\dot{y}}$ (m/sec)	.558		.317
σ_{δ_A} (m)	.00414		.00335
σ_{δ_P} (m)	.000940		.000721
Probability of remaining within Category II window	.979	.994	.999

TABLE VI.- SIMPLIFIED FORMS OF DOMINANT PILOT TRANSFER FUNCTIONS

Longitudinal	Lateral
Baseline	
$\frac{\delta_E}{u} = \frac{-0.00404}{(s+1.0)} G(s)^a \frac{m}{m/sec}$	$\frac{\delta_A}{\sigma} = \frac{-0.149(s+0.15)}{(s+0.8)^2} G(s)$ m/rad
$\frac{\delta_E}{\theta} = \frac{0.043}{(s+1.0)} G(s)$ m/rad	$\frac{\delta_A}{\psi} = \frac{-0.0328\ s}{(s+0.8)^2} G(s)$ m/rad
$\frac{\delta_C}{h} = \frac{-0.00630(s+0.35)}{(s+0.17)(s+2.0)} G(s)$ m/m	$\frac{\delta_A}{y} = \frac{-0.000195(s+0.25)}{(s+0.8)^2} G(s)$ m/m
$\frac{\delta_C}{\gamma} = \frac{-0.159(s+0.65)}{(s+0.17)(s+2.0)} G(s)$ m/rad	$\frac{\delta_P}{\sigma} = \frac{-0.0116\ (s-0.2)}{(s+0.2)(s+0.5)} G(s)$ m/rad
	$\frac{\delta_P}{\psi} = \frac{-0.00636(s-0.2)}{(s+0.2)(s+3.5)} G(s)$ m/rad
	$\frac{\delta_P}{\dot{\psi}} = \frac{-0.0212}{(s+3.5)} G(s) \frac{m}{rad/sec}$
Stab-Aug	
$\frac{\delta_E}{h} = \frac{-0.00380}{(s+0.35)(s+3.0)} G(s)$ m/m	lateral same as Baseline
$\frac{\delta_E}{\gamma} = \frac{-0.168}{(s+0.35)(s+3.0)} G(s)$ m/rad	
$\frac{\delta_C}{h} = \frac{-0.00620}{(s+0.7)} G(s)$ m/m	
$\frac{\delta_C}{\gamma} = \frac{-0.296}{(s+0.7)} G(s)$ m/rad	

[a] $G(s) = e^{-0.2s}/(0.2s + 1)$ and represents the pilot's effective time delay and neuromuscular dynamics.

TABLE VII.- OBSERVED VARIABLES AND DISPLAY GAINS FOR FLIGHT DIRECTOR STUDY

Definition	Variable	Maximum allowable deviation	Display gain
Longitudinal			
Longitudinal cyclic director	d_1	0.0381 m (0.125 ft)	17.5 cm/m
Collective director	d_2	.0381 m	17.5 cm/m
Lateral			
Lateral cyclic director	d_3	0.0381 m	17.5 cm/m
Lateral flight path angle error	σ	.0873 rad	7.62 cm/rad
	$\dot{\sigma}$	.0873 rad/sec	7.62 $\frac{\text{cm/sec}}{\text{rad/sec}}$
Heading error	ψ	.0873 rad	7.62 cm/rad
	$\dot{\psi}$	.0873 rad/sec	7.62 $\frac{\text{cm/sec}}{\text{rad/sec}}$

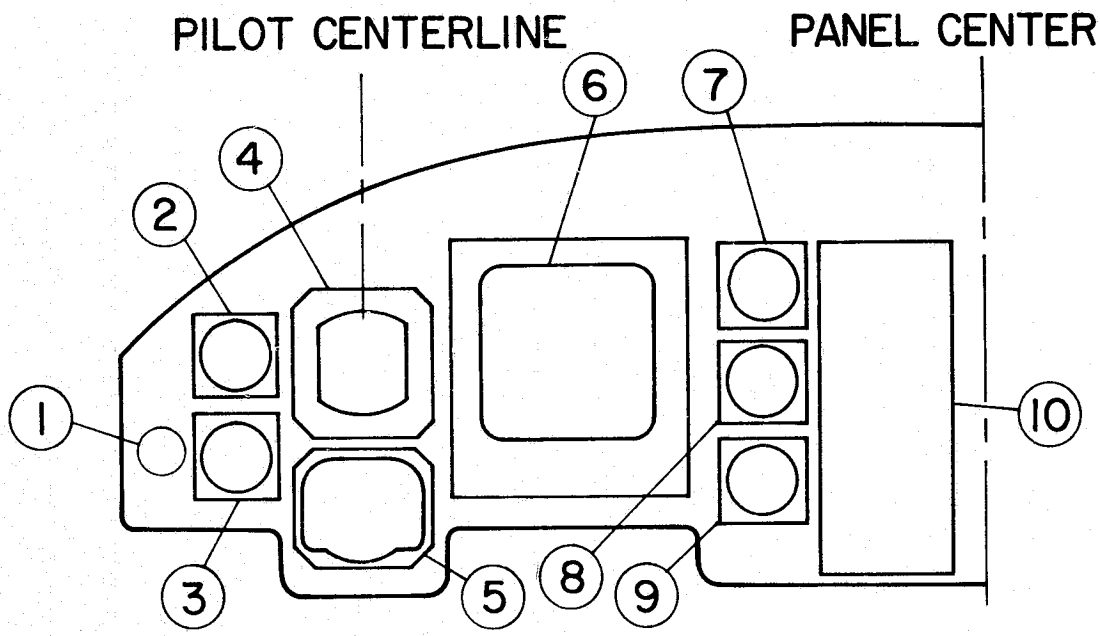

1. TORQUEMETER
2. TRUE AIRSPEED INDICATOR
3. DUAL-TACHOMETER
4. ATTITUDE DIRECTOR INDICATOR (ADI)
5. HORIZONTAL SITUATION INDICATOR (HSI)
6. MULTIFUNCTION DISPLAY (MFD)
7. BAROMETRIC ALTIMETER
8. VERTICAL SPEED INDICATOR
9. RADIO ALTIMETER
10. MODE SELECT PANEL

Figure 1.- UH-1H V/STOLAND pilot control panel.

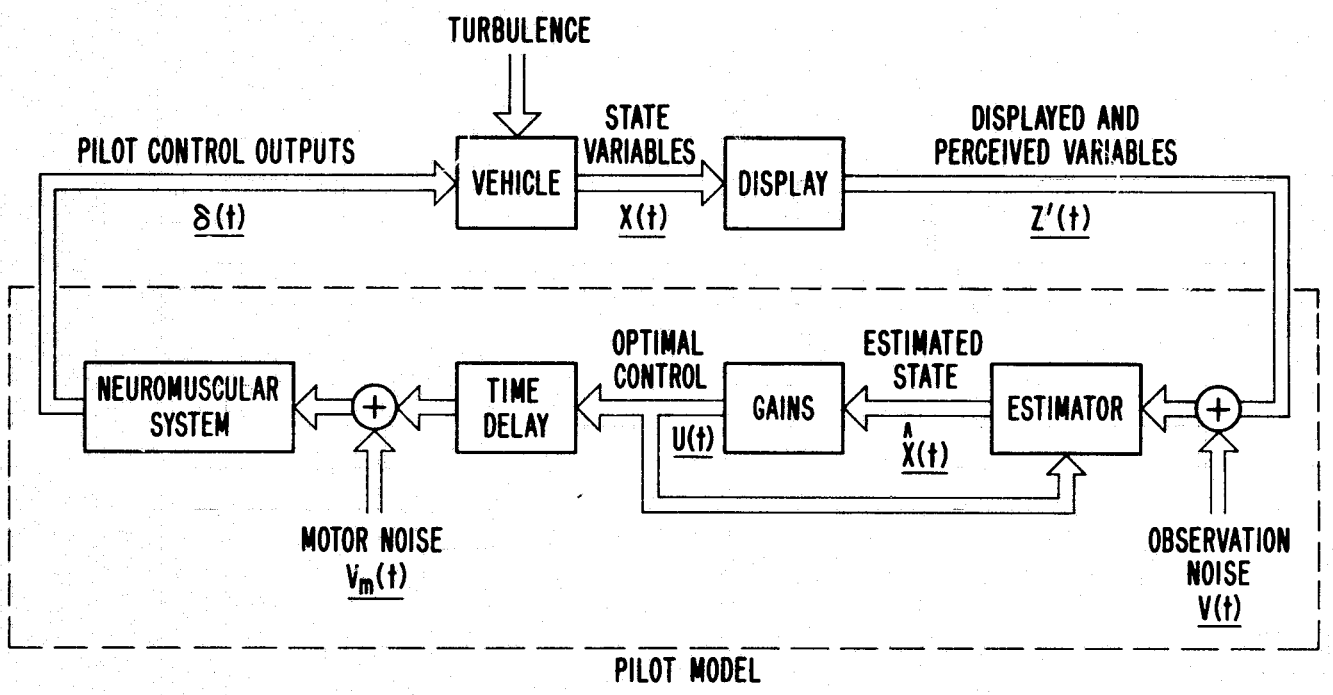

Figure 2.- Block diagram of pilot/vehicle system.

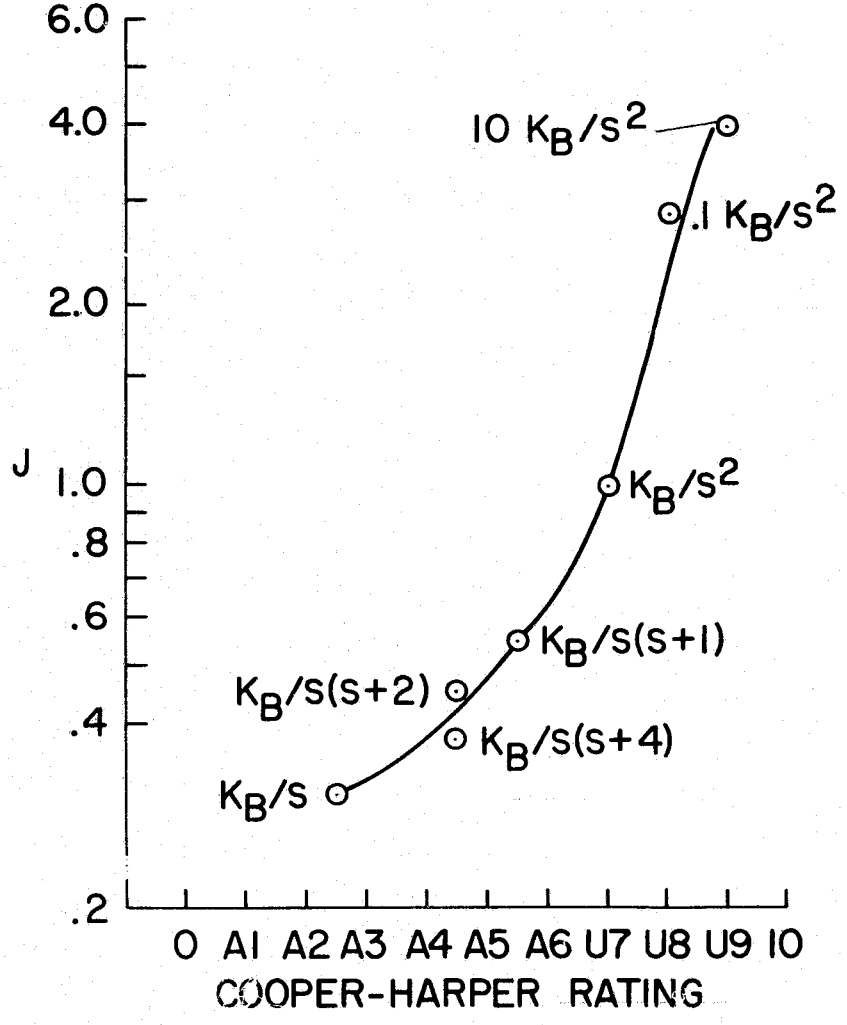

Figure 3.- Rating curve for Cooper-Harper rating scale.

CONTROLLABLE CAPABLE OF BEING CONTROLLED OR MANAGED IN CONTEXT OF MISSION, WITH AVAILABLE PILOT ATTENTION.	ACCEPTABLE MAY HAVE DEFICIENCIES WHICH WARRANT IMPROVEMENT, BUT ADEQUATE FOR MISSION. PILOT COMPENSATION, IF REQUIRED TO ACHIEVE ACCEPTABLE PERFORMANCE, IS FEASIBLE.	SATISFACTORY MEETS ALL REQUIREMENTS AND EXPECTATIONS, GOOD ENOUGH WITHOUT IMPROVEMENT. CLEARLY ADEQUATE FOR MISSION.	EXCELLENT, HIGHLY DESIRABLE.	A1
			GOOD, PLEASANT, WELL BEHAVED.	A2
			FAIR. SOME MILDLY UNPLEASANT CHARACTERISTICS. GOOD ENOUGH FOR MISSION WITHOUT IMPROVEMENT.	A3
		UNSATISFACTORY RELUCTANTLY ACCEPTABLE. DEFICIENCIES WHICH WARRANT IMPROVEMENT. PERFORMANCE ADEQUATE FOR MISSION WITH FEASIBLE PILOT COMPENSATION.	SOME MINOR BUT ANNOYING DEFICIENCIES. IMPROVEMENT IS REQUESTED. EFFECT ON PERFORMANCE IS EASILY COMPENSATED FOR BY PILOT.	A4
			MODERATELY OBJECTIONABLE DEFICIENCIES. IMPROVEMENT IS NEEDED. REASONABLE PERFORMANCE REQUIRES CONSIDERABLE PILOT COMPENSATION.	A5
			VERY OBJECTIONABLE DEFICIENCIES. MAJOR IMPROVEMENTS ARE NEEDED. REQUIRES BEST AVAILABLE PILOT COMPENSATION TO ACHIEVE ACCEPTABLE PERFORMANCE.	A6
	UNACCEPTABLE DEFICIENCIES WHICH REQUIRE MANDATORY IMPROVEMENT. INADEQUATE PERFORMANCE FOR MISSION EVEN WITH MAXIMUM FEASIBLE PILOT COMPENSATION.		MAJOR DEFICIENCIES WHICH REQUIRE MANDATORY IMPROVEMENT FOR ACCEPTANCE. CONTROLLABLE. PERFORMANCE INADEQUATE FOR MISSION, OR PILOT COMPENSATION REQUIRED FOR MINIMUM ACCEPTABLE PERFORMANCE IN MISSION IS TOO HIGH.	U7
			CONTROLLABLE WITH DIFFICULTY. REQUIRES SUBSTANTIAL PILOT SKILL AND ATTENTION TO RETAIN CONTROL AND CONTINUE MISSION.	U8
			MARGINALLY CONTROLLABLE IN MISSION. REQUIRES MAXIMUM AVAILABLE PILOT SKILL AND ATTENTION TO RETAIN CONTROL.	U9
UNCONTROLLABLE CONTROL WILL BE LOST DURING SOME PORTION OF MISSION.			UNCONTROLLABLE IN MISSION	10

Figure 4.- The revised Cooper-Harper scale.

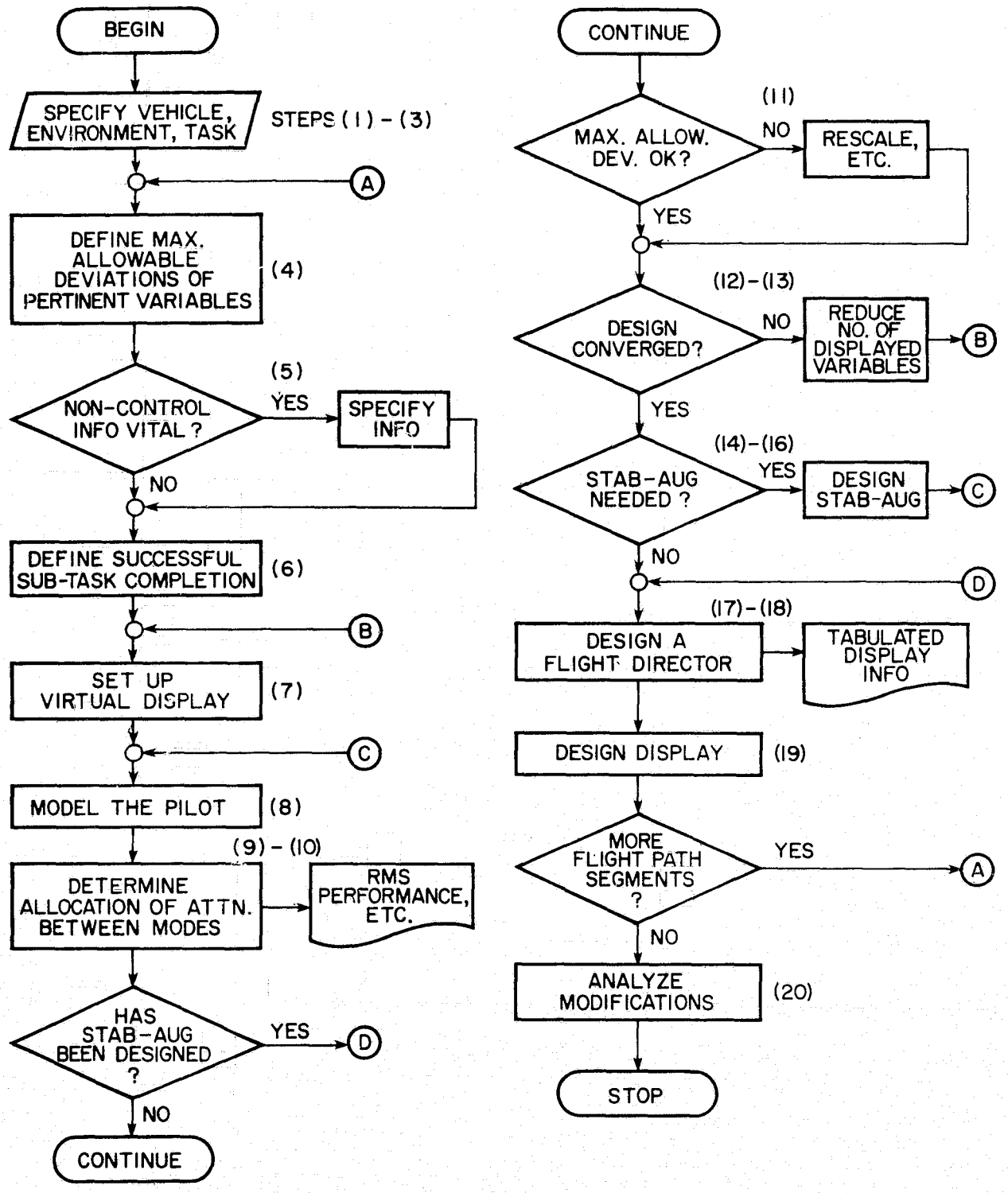

Figure 5.- Flow chart for display design.

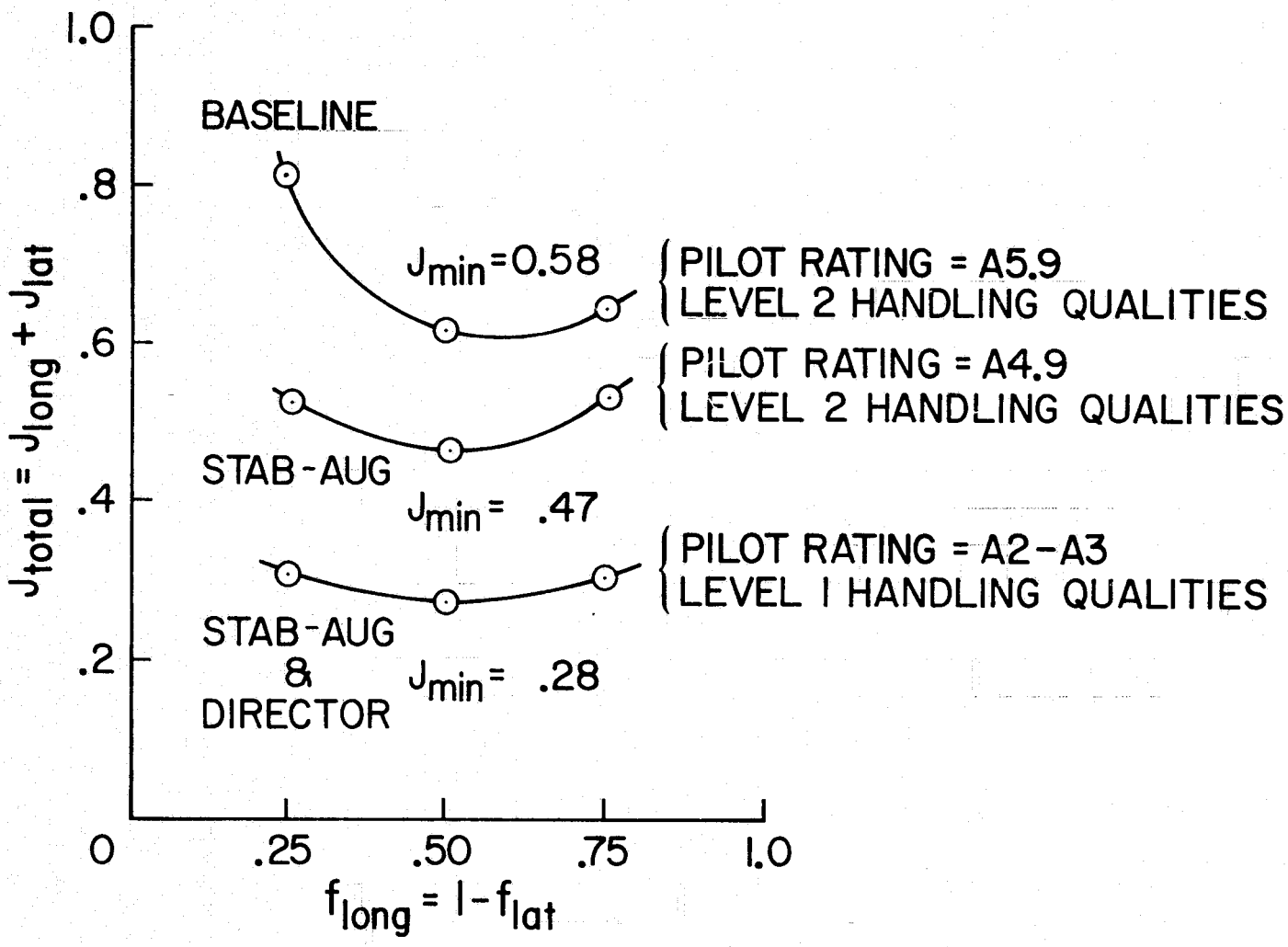

Figure 6.- Value of model index of performance vs fraction of attention on longitudinal (lateral) task.

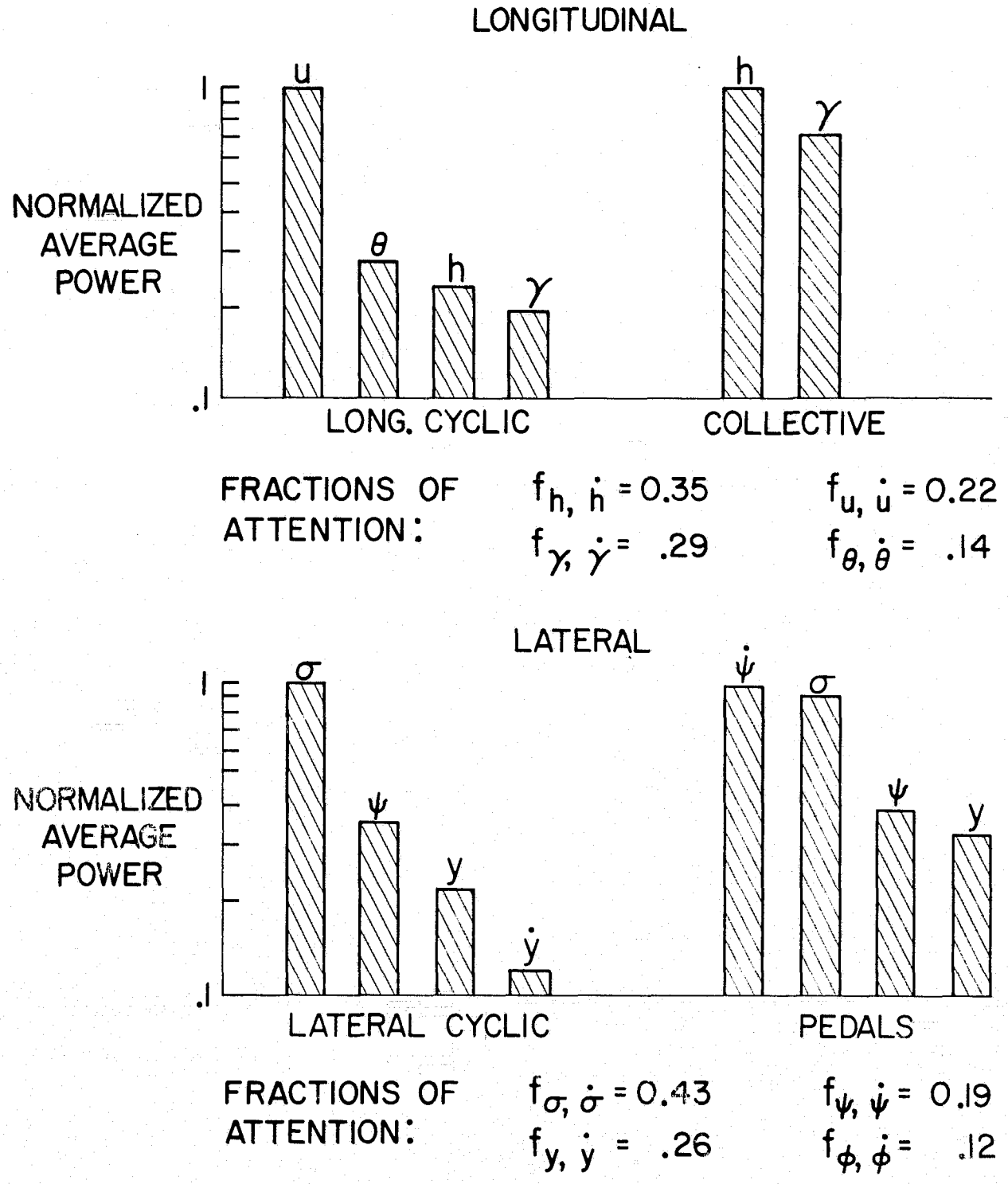

Figure 7.- Normalized average power and fractions of attention for Baseline configuration.

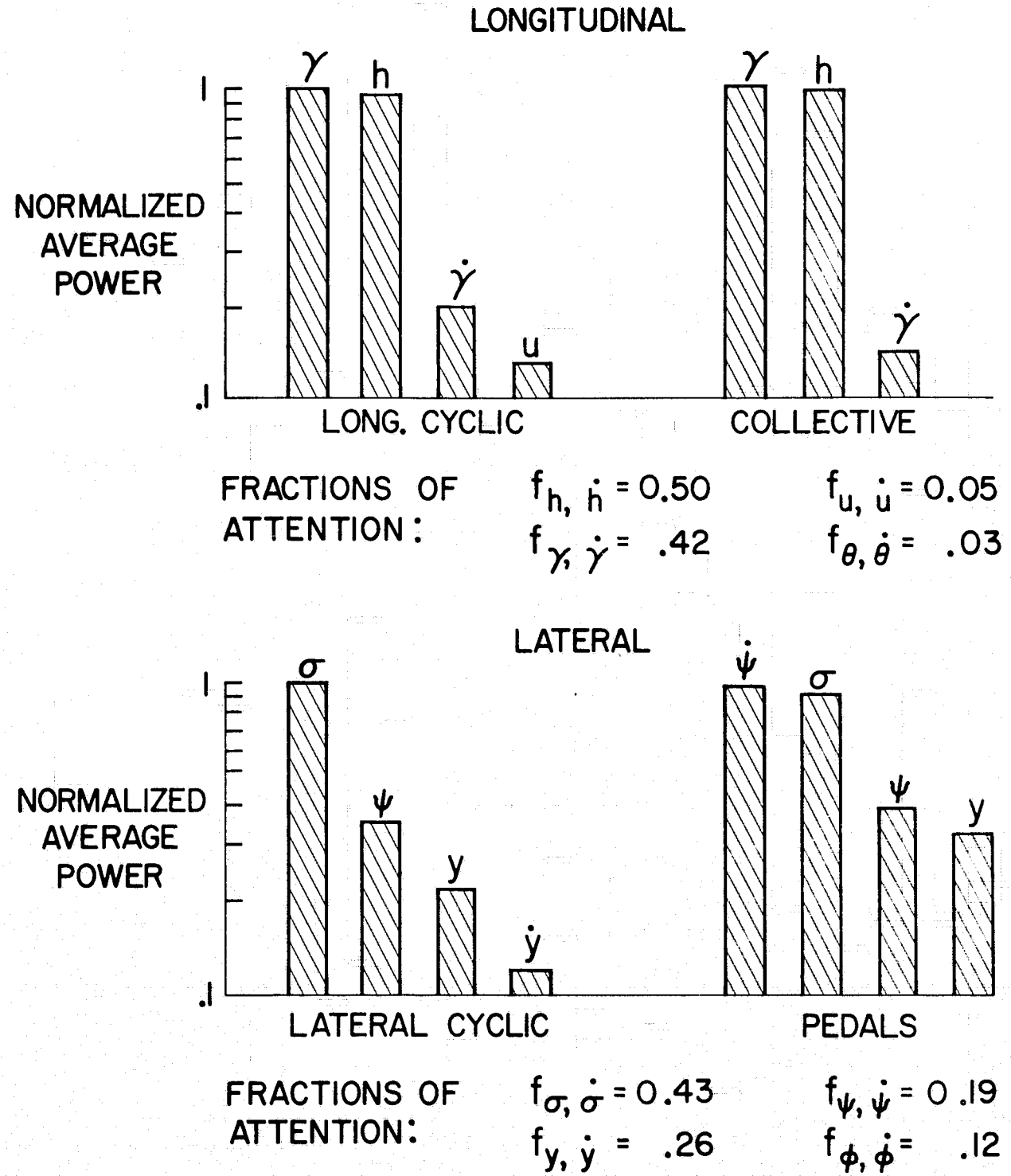

Figure 8.- Normalized average power and fractions of attention for Stab-Aug configuration.

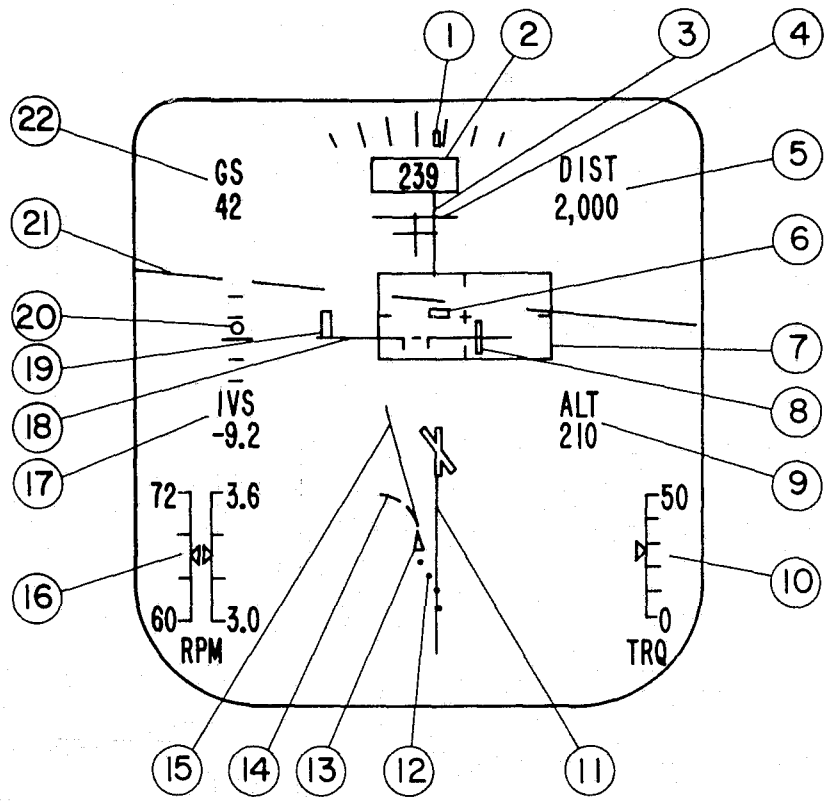

1. ROLL INDICATOR
2. DIGITAL HEADING READOUT (deg)
3. LATERAL CYCLIC DIRECTOR BAR
4. LONGITUDINAL CYCLIC DIRECTOR BAR
5. DISTANCE-TO-GO DIGITAL READOUT (ft)
6. LONGITUDINAL (γ) AND LATERAL (σ) FLIGHT PATH ANGLE ERROR
7. GLIDESLOPE ERROR (h) AND COURSE ERROR (y) "WINDOW"
8. HEADING ERROR
9. ALTITUDE DIGITAL READOUT (ft)
10. TORQUEMETER (psi)
11. HORIZONTAL SITUATION INDICATOR (HSI) EXTENDED RUNWAY CENTERLINE
12. HSI GROUND TRACK HISTORY
13. FIXED AIRCRAFT SYMBOL (HEADING UP)
14. TRACK PREDICTOR
15. COURSE VECTOR
16. DUAL-TACHOMETER (RPM)
17. INSTANTANEOUS VERTICAL SPEED DIGITAL READOUT (ft/sec)
18. FIXED AIRCRAFT SYMBOL
19. GROUNDSPEED ERROR (u)
20. COLLECTIVE DIRECTOR "DOUGHNUT"
21. ARTIFICIAL HORIZON (θ & ϕ)
22. GROUNDSPEED DIGITAL READOUT (knots)

Figure 9.- Candidate V/STOLAND display.

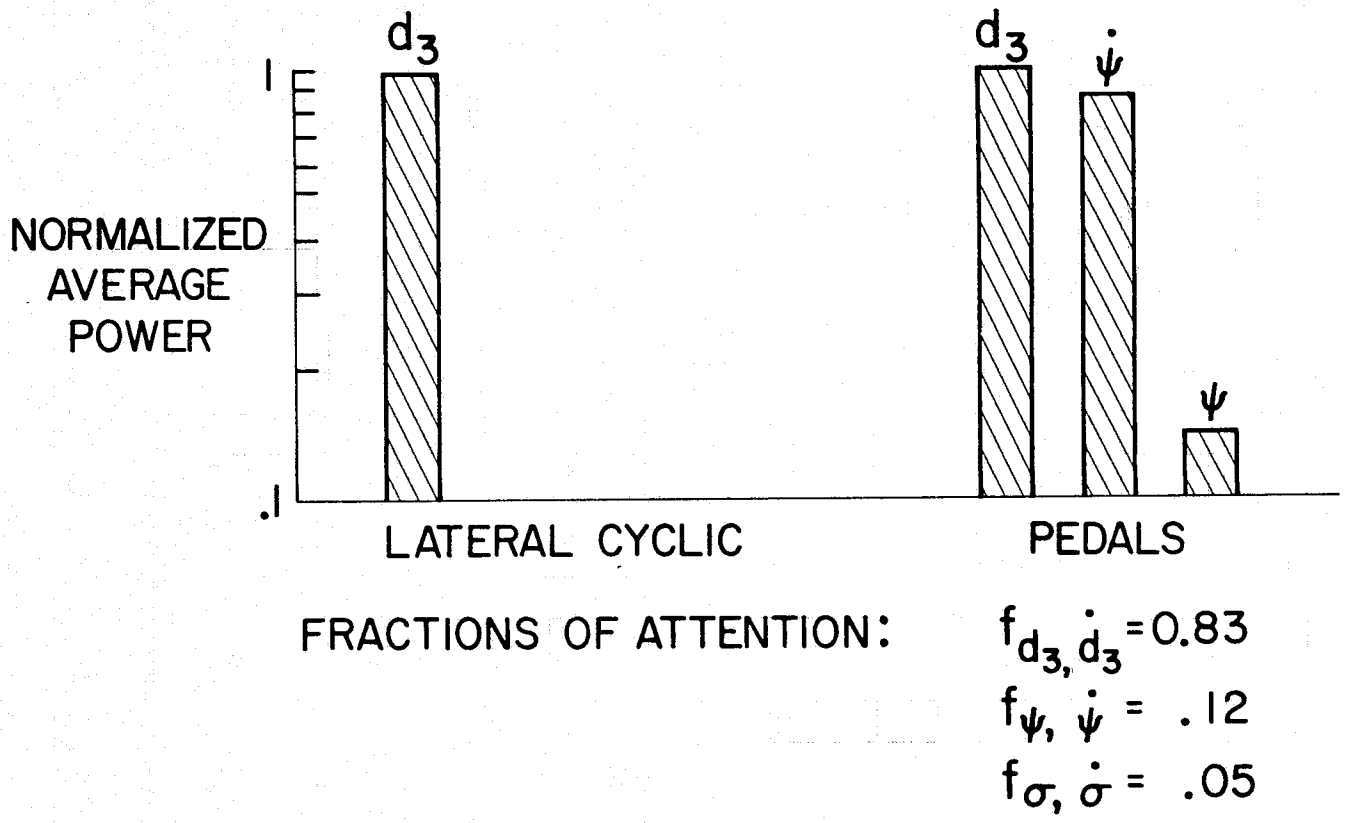

Figure 10.- Normalized average power and fractions of attention for lateral Director configuration.